Local Bifurcation in Power Systems: Theory, Computation, and Application

HARRY G. KWATNY, SENIOR MEMBER, IEEE, ROBERT F. FISCHL, LIFE FELLOW, IEEE, AND CHIKA O. NWANKPA, MEMBER, IEEE

Invited Paper

This paper provides an overview of local bifurcation theory and its application to power system voltage stability analysis. The qualitative behavior of power system dynamics as modeled by differential-algebraic equations is discussed, followed by a summary of the concepts and tools for the analysis of local bifurcation from equilibria. Computational methods for locating and classifying bifurcation points as they have been applied in power system analysis are reviewed. Several examples are given.

I. INTRODUCTION

During the past decade power system engineers have had to seriously confront issues imposed by increased reliance on power transfer over long distances. Difficulty in controlling bus voltages, noncovergence of load flow calculations and small transient stability domains are just some of the problems routinely encountered. The essential fact is that transmission systems now operate well outside of a linear domain so that planning and operations must address power system nonlinear behavior. There is a need for analytical concepts and tools that work when nonlinearity is critical.

In this paper we address the simplest class of problems in nonlinear dynamics—behaviors that can be completely characterized locally. That is, in a neighborhood (not necessarily small) of some operating point. Local bifurcations are readily evident in power systems as important elements of voltage instability. The two most elementary of these—the saddle-node and the Hopf bifurcations—have received, by far, most of the attention. We discuss these and other local bifurcations in this paper. It is quite likely that time will demonstrate the importance of global bifurcations in formulating a complete understanding of power system stability issues and of routes to voltage collapse [1], [2].

The main goal of this paper is to provide an overview of local bifurcation theory as it applies to power systems—emphasizing the unique aspects of power systems and summarizing the substantial literature that has developed during the past decade. Because power systems are very large scale systems, computational questions are always a foremost concern and we will address some of them. The influence that bifurcation theory has already had in clarifying voltage stability issues and motivating the development of new computational tools is actually quite remarkable. There is a definite opportunity and a need to consolidate what has been learned about power system nonlinear behavior in a form that will encourage and facilitate a broader assimilation of these results within the power engineering community.

Our formulation is fairly general. We view a power system as a set of parameter dependent differential and algebraic equations (DAE's) and discuss the (local) static and dynamic behavior of such systems as a function of the parameters. The paper is organized in two main parts. Section II summarizes the qualitative theory, and Section III deals with computational methods and examples. In Section II we discuss the qualitative behavior associated with DAE models and give an example of a simple power system that exhibits many of their distinctive features. Also, in Section II, we summarize the main elements of local bifurcation theory in the framework of DAE models.

In Section III, we consider the two central computational issues: the location and classification of local bifurcation points. Most of the emphasis is placed on variants of the Newton–Raphson–Seydel method and continuation methods for the former and the Lyapunov–Schmidt method for the latter. We explain how these techniques can be used to analyze both static and dynamic (Hopf) bifurcations. Examples given in Section III serve several purposes. Of course, they illustrate application of the numerical tools but more importantly, they demonstrate the power of the concepts behind the computations. The complexity of behavior exhibited by power systems requires some organizational framework within which to comprehend it.

Manuscript received August 12, 1994; revised September 1, 1995.

H. G. Kwatny is with the Mechanical Engineering Department, Drexel University, Philadelphia, PA 19104 USA.

R. F. Fischl and C. O. Nwankpa are with the Electrical Engineering Department, Drexel University, Philadelphia, PA 19104 USA.

IEEE Log Number 9415382.

The examples also, we hope, give physical meaning to some of the more subtle theoretical concepts.

Since the recent literature pertaining to the subject of this paper is quite extensive, our reference list necessarily omits many interesting papers. Nevertheless, we hope that we have provided sufficient connections to the literature to give a motivated reader a good start. We are particularly indebted to a few pioneers who asked crucial questions in the 1970's and earlier—before the significance of the issues they raised was widely appreciated—and whose papers clearly shaped current thinking, notably: Tavora and Smith [3], [4], Korsac [5], and Venikov *et al.* [6].

II. Qualitative Properties of Power System Dynamics

A. Power Systems as Differential-Algebraic Dynamical Systems

Mathematical models of power systems generally consist of a set of parameter dependent differential and algebraic equations (DAE's) in the form

$$\begin{aligned} \dot{x} &= f(x, y, \mu) \\ 0 &= g(x, y, \mu) \end{aligned} \tag{1}$$

where $x \in R^n$, and $y \in R^m$ denote the system dependent variables, $\mu \in R^p$ denotes a vector of system parameters, and f: $R^{n+m+p} \rightarrow R^n, g$: $R^{n+m+p} \rightarrow R^m$, are smooth $(C^k, k \geq 1)$ functions. For example, the classical model composed of n_g generators, n_{PV} PV load buses and n_{PQ} PQ load buses is commonly expressed

$$\begin{aligned} \dot{\delta} &= \omega \\ M\dot{\omega} + D\omega + f_g(\delta, \theta, V, \mu) &= 0 \\ f_l(\delta, \theta, V, \mu) &= 0 \end{aligned} \tag{2}$$

with $\omega, \delta \in R^{n_g}$, $\theta \in R^{n_{PQ}+n_{PV}}$, and $V \in R^{n_{PQ}}$. Since $\det(M) \neq 0$, (2) is clearly of the type (1). However, (1) admits various enhancements to the classical model including excitation systems, tap changing transformers, nonlinear and dynamic loads, and more elaborate generator models [7]–[12]. While (2) is an important special case of (1) to which we shall make frequent reference, our development is based on (1).

Equilibria of (1) satisfy the algebraic equations

$$\begin{aligned} 0 &= f(x, y, \mu) \\ 0 &= g(x, y, \mu). \end{aligned} \tag{3}$$

We will refer to the equilibrium equations (3) as the 'load flow' equations. The importance of consistent dynamic and static (equilibrium) models cannot be overstated. Sometimes in practice, power system dynamic analysis and load flow analysis utilize models developed by different modelers and based on different assumptions. As an unfortunate consequence there may arise an artificial distinction between static and dynamic phenomenon. In fact, while it is essential to study the solution structure of (3), any interesting 'static' behavior exhibited by it, is directly linked to corresponding 'dynamic' behavior of (1).

We wish to emphasize two essential features of the model (1): 1) the explicit parameter dependence, and 2) the differential-algebraic structure.[1] Consideration of the change in system behavior that occurs as a consequence of parameter variation is the main theme of this paper. Indeed, this perspective is the key to formulating concepts of stability that allow systematic examination of voltage collapse phenomenon. In addition to the obvious computational issues, a differential-algebraic structure can produce behaviors not present in purely differential equations [14], [18]. For instance, if the classical system (2) contains only constant admittance loads (no constant power loads) then it is equivalent to a purely differential system. In this case parametrically induced instabilities are present, but these are 'steady-state' (or angle) instabilities. 'Voltage collapse'—in the customary sense—does not occur.[2] We will elaborate on these points below.

Systems described by DAE's are frequently encountered in engineering and are studied as dynamical systems that evolve on manifolds. An insightful introduction to this point of view is the discussion of nonlinear RLC circuits in [19, Chap. 10]. Numerical methods for solving DAE's and other examples and references may be found in [20]. We will outline the conceptual framework within which (1) is to be considered and then provide a power system example that illustrates the main issues.

Note that the algebraic part of (1), $0 = g(x, y, \mu)$, requires that any motion be constrained to the set

$$\mathcal{M} = \{(x, y) \in R^{n+m} \mid 0 = g(x, y, \mu), \mu = \text{const}\}. \tag{4}$$

Typically, we expect $\mathcal{M}$ to be composed of one or more disconnected (differentiable) manifolds[3] [22] called components. In general, when we refer to $\mathcal{M}$ we will mean a particular one of these components called the *principal component*. $\mathcal{M}$ is a *regular* manifold of dimension n if

$$\operatorname{rank}\left[\frac{\partial g}{\partial x}\frac{\partial g}{\partial y}\right] = m \text{ on } \mathcal{M}. \tag{5}$$

The structure of $\mathcal{M}$ depends, of course, on the parameter μ. Even for very simple power system models (5) may not be satisfied for some values of μ.

[1] Some investigators have cautioned that there are often underlying dynamics associated with alebraic constraints so that peculiarities associated with DAE models should be interpreted with accordant care [13]–[16]. Often algebraic equations arise by neglecting underlying dynamics which are fast and stable. This may be done formally via singular perturbations [17] or at the level of formulation of the governing equations. Questions of validity of any such approximations are beyond the scope of this paper.

[2] This does not imply that DAE models are necessary to exhibit voltage instability. Differential equation models with appropriate dynamic loads would do so.

[3] An m-dimensional *manifold* $\mathcal{M} \subset R^n$ is a set for which each $x \in \mathcal{M}$ has a neighborhood U for which there is a smooth, invertible mapping ϕ: $R^m \rightarrow U(m \leq n)$ [21]. A manifold is usually defined by an 'embedding' relation, $g(x) = 0$, g: $R^n \rightarrow R^{n-m}$, or 'parametrically' by a map from a parameter space π: $R^m \rightarrow R^n$.

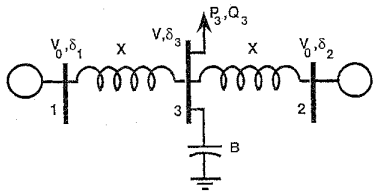

Fig. 1. This simple network nicely illustrates some essential properties of power systems described by DAE's.

The manifold $\mathcal{M}$ is the *state space* for the dynamical system defined by (1) which induces a vector field on $\mathcal{M}$. The vector field may not be well defined at all points of $\mathcal{M}$. At any point $(x, y) \in \mathcal{M}$ we have $\dot{x} = f(x, y, \mu)$. If $\det[\partial g/\partial y] \neq 0$, then $\dot{y}$ is uniquely defined by

$$\dot{y} = -\left[\frac{\partial g}{\partial y}\right]^{-1} \frac{\partial g}{\partial x}\dot{x}. \tag{6}$$

If this is the case, it is easy to show that the velocity vector defined by $\dot{x}$ and $\dot{y}$ is tangent to $\mathcal{M}$ at (x, y). If $\partial g/\partial y$ is singular at a point $(x, y) \in \mathcal{M}$ then the vector field is not well defined at that point. Typically, such singular points lie on codimension[4] 1 submanifolds of $\mathcal{M}$. In power systems such points were encountered by DeMarco and Bergen [13] in connection with transient stability studies ('impasse' points),[5] by Kwatny *et al.* [14] in connection with bifurcation analysis ('noncausal' points) and others ('impasse surfaces' in [24]; 'singularity' in [25]).

Definition 1: Suppose $\mathcal{M}$ is a regular manifold for all μ near μ^*, and that $\det[\partial g/\partial y] \neq 0$ at a point $\mu = \mu^*$, $(x, y) = (x^*, y^*) \in \mathcal{M}$. Then (x^*, y^*, μ^*) is said to be *causal*. Otherwise it is *noncausal*.

If (x^*, y^*, μ^*) is causal, then the Implicit Function Theorem ensures that there exists a function $\psi(x, \mu)$ defined on a neighborhood of (x^*, μ^*), with $y^* = \psi(x^*, \mu^*)$ and that satisfies $g(x, \psi(x, \mu), \mu) = 0$. It follows that near the causal point (x^*, y^*, μ^*), the trajectories of the DAE (1) are locally defined by the ordinary differential equation

$$\dot{x} = \phi(x, \mu) := f(x, \psi(x, \mu), \mu). \tag{7}$$

Example 1: (A Simple Three-Bus Network): The network shown in Fig. 1 was used in [14] to illustrate some of the properties of power systems described by DAE's. Although extremely simple, configurations like this involving one or two generators feeding a remote load have often been used in discussions of voltage stability and control [26]–[30].

Suppose that P_1, P_2, P_3, denote the bus real power injections. Equilibrium solutions exist only if $P_1 + P_2 + P_3 = 0$. We assume that this is the case. For convenience, fix some of the parameters: $V_0 = 1$, $X = 1$, $M_1 = 1$, $M_2 = 1$, where M_1, M_2 are the generator inertia constants, and let $\theta = \delta_2 - \delta_1$, $\phi = \delta_3 - \delta_1$, and $\Delta P = P_2 - P_1$. The equations of motion are then

$$\begin{aligned} \ddot{\theta} &= -V\sin(\theta - \phi) - V\sin\phi + \Delta P \\ 0 &= V(\sin\phi + \sin(\phi - \theta)) - P_3 \\ 0 &= -V(\cos\phi + \cos(\phi - \theta)) + (2 - B)V^2 - Q_3. \end{aligned}$$

Any motion is constrained by the two algebraic equations. Within the three dimensional (3-D) space of independent varables (θ, ϕ, V) these equations define a one-dimensional (1-D) manifold called a *configuration* manifold. Each point on this configuration manifold has a 1-D tangent space. When these are collected together, they form a two dimensional (2-D) state space (called the *tangent bundle*). Clearly, the configuration manifold, and hence the state space, can change its shape as the system parameters vary.

In [14] it is shown that for almost all values of the parameters the configuration space is a closed curve so that the state space is topologically equivalent to a cylinder. Moreover, the noncausal points form two 1-D submanifolds that divide the cylinder into two sheets. The parameter dependence of the system equilibria is investigated for various values of ΔP while the remaining parameters are fixed: $P_3 = -1$, $Q_3 = 0$, $B = 1$. As ΔP is decreased from 0 to -1, the system has two stable equilibria which move as indicated in Fig. 2. As ΔP decreases below -1, the left equilibrium moves through the noncausal set into the adjacent sheet and becomes unstable. Further decreases in ΔP cause the two equilibria to meet and annihilate each other. As shown in [14], if the parameter B is reduced with all others held fixed, then the "radius" of the cylindrical state space decreases so that the state space shrinks to a line as $B \to 0$.

Another, and quite different, example of a power system with DAE description is given in [18], [25]. Here again, a 2-D state space is divided by a 1-D submanifold of noncausal points. The analysis in [18], [25] illustrates a one-parameter variation that causes an equilibrium point to cross the noncausal set and shows that the crossing is accompanied by an exchange of stability of one eigenvalue that diverges through infinity. This is called a singularity-induced bifurcation.

B. Equilibria

1) Equilibria: As we have noted, an equilibrium point of (1) is a point (x^*, y^*, μ^*) that satifies (3). We need to examine this idea in more detail. First, let $\mathcal{G}$ denote the set of points that satisfy the relation $g(x, y, \mu) = 0$

$$\mathcal{G} = \{(x, y, \mu) \in R^{n+m+p} \mid 0 = g(x, y, \mu)\}. \tag{8a}$$

This set forms a regular manifold of dimension $n + p$ in R^{n+m+p} provided

$$\operatorname{rank}\left[\frac{\partial g}{\partial x}\frac{\partial g}{\partial y}\frac{\partial g}{\partial \mu}\right] = m \text{ on } \mathcal{G}. \tag{8b}$$

[4]The *codimension* of a k-dimensional submanifold of an n-dimensional manifold is $n - k$ [21].

[5]Impasse points can arise from a mechanism quite different from the situation here [23], so we will not use this terminology.

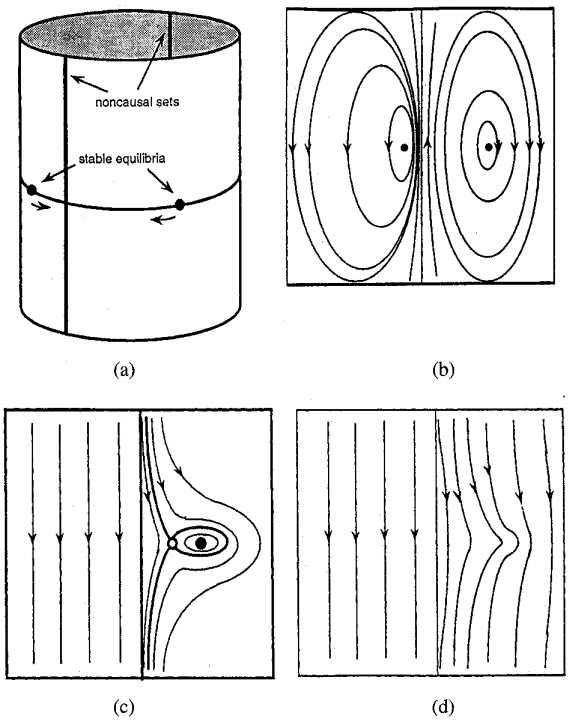

Fig. 2. (a) The cylindrical state space is divided into two sheets by the noncausal sets or "impasse" surfaces. (b) The cylindrical space is flattened out in order to illustrate the state trajectories on the two sheets. (c) As ΔP decreases below -1, the left equilibrium point migrates into the right sheet and changes from stable to unstable. (d) Further decreases in ΔP causes a bifurcation that leaves no equilibria. The post-bifurcation trajectories are illustrated here.

Similarly, the set

$$\mathcal{F} = \{(x, y, \mu) \in R^{n+m+p} \mid 0 = f(x, y, \mu)\} \tag{9a}$$

forms a regular manifold of dimension $m + p$ in R^{n+m+p} provided

$$\operatorname{rank}\left[\frac{\partial f}{\partial x}\frac{\partial f}{\partial y}\frac{\partial f}{\partial \mu}\right] = n \text{ on } \mathcal{F}. \tag{9b}$$

Equilibria are the points in the intersection of these manifolds. We will assume a transversal intersection of $\mathcal{F}$ and $\mathcal{G}$. Otherwise an arbitrarily small perturbation in either f or g will cause it to be transversal. A transversal intersection implies that either $\mathcal{F}$ and $\mathcal{G}$ do not intersect at all or the intersection forms a regular p-dimensional submanifold of R^{n+m+p} (and, of course, $\mathcal{F}$ and $\mathcal{G}$).[6]

2) Basic Assumptions: In the following, we will assume (8b), (9b), and a transversal intersection of $\mathcal{F}$ and $\mathcal{G}$.

Notice that our basic assumptions do not imply either

$$\operatorname{rank}\left[\frac{\partial g}{\partial x}\frac{\partial g}{\partial y}\right] = m \text{ on } \mathcal{G} \tag{10a}$$

or

$$\operatorname{rank}\left[\frac{\partial f}{\partial x}\frac{\partial f}{\partial y}\right] = n \text{ on } \mathcal{F}. \tag{10b}$$

[6]For a discussion and definitions of transversal intersections, see [31].

We have already noted that (10a) ensures that the state space is a regular n-dimensional manifold. There may be meaningful instances in power systems where (10a) can fail. Clearly, failure of (10a) automatically implies noncausality, but its implications are deeper than that, indicating a degeneracy of the underlying state space geometry.

Failure of either (10a or b) at equilibria are special cases of static bifurcations to be considered below. We will not attach special significance to these bifurcations beyond what has already been said [32], [33].

3) Stability of Equilibria: The concept of stability in the sense of Lyapunov applies generally to flows on manifolds and, in particular, it applies to equilibria of DAE's. Thus an equilibrium point of (1) is stable if it is stable in the sense of Lyapunov. This concept of stability can be useful even for noncausal equilibria. We will not develop these ideas here. If the equilibrium point is causal, then (7) defines the flow near it, so that classical notions of stability of equilibria of vector fields apply. We will summarize some important concepts for this case.

4) Hartman–Grobman: Consider the ordinary differential equation

$$\dot{x} = \phi(x), x \in R^n \tag{11}$$

with equilibrium point at the origin, $\phi(0) = 0$. Let $A := D_x\phi(0)$. We wish to know how much information about the behavior of (11) near the origin can be determined from its linearization. The answer is given by the following theorem [21], [34].

Theorem 1 (Hartman–Grobman Theorem): If A has no eigenvalues on the imaginary axis, then there is a continuous map with continuous inverse h defined on some neighborhood U of the origin in R^n locally taking trajectories of the flow defined by (11) to those of the linear flow $e^{At}x$. The mapping preserves the sense of time and can be chosen to preserve the parameterization of time.

Equilibria for which A has no eigenvalues on the imaginary axis are called *hyperbolic*. The theorem guarantees that the stability of hyperbolic equilibria can be determined from the linearization of the vector field. But it does much more than that by establishing the local equivalence of the nonlinear and linear flows.

Let us describe what this equivalence means. Recall that for a linear system with a hyperbolic equilibrium point we can define the eigenspaces E^s, E^u corresponding to the eigenvalues with negative real parts and positive real parts respectively, and the behavior of the system can be completely characterized in terms of the motion on these subspaces. For a nonlinear system with a hyperbolic equilibrium point there are correspondingly (local) stable and unstable manifolds W^s, W^u of the same dimension as, and tangent to E^s, E^u at the equilibrium point. Equally important is the fact that 'small' perturbations of the function ϕ in (11) will not alter the dimensions of E^s, E^u or W^s, W^u [35].

5) The Center Manifold: Local behavior of (11) near a nonhyperbolic equilibrium point is not completely

characterized by its linearization. The following important theorem explains the general case.

Theorem 2 (Center Manifold Theorem): Consider (11) with ϕ a C^k function,[7] an equilibrium point at the origin, $\phi(0) = 0$ and with $A := D_x\phi(0)$. Let the spectrum of A be divided into three sets $\sigma_s, \sigma_c, \sigma_u$ with

$$\operatorname{Re}\lambda = \begin{cases} < 0 & \text{if } \lambda \in \sigma_s \\ = 0 & \text{if } \lambda \in \sigma_c \\ > 0 & \text{if } \lambda \in \sigma_u \end{cases}.$$

Let the (generalized) eigenspaces of $\sigma_s, \sigma_c, \sigma_u$ be E^s, E^c, E^u, respectively. Then there exist C^k stable and unstable manifolds W^s and W^u tangent to E^s and E^u, respectively, at $x = 0$ and a C^{k-1} center manifold W^c tangent to E^c at $x = 0$. The manifolds W^s, W^c, and W^u are all invariant[8] with respect to the flow of (11). The stable and unstable manifolds are unique, but the center manifold need not be.

Notice that the theorem decomposes the local flow into three parts: a flow on the stable manifold (trajectories converge to the origin), a flow on the unstable manifold (trajectories diverge from the origin) and flow on the center manifold (the behavior of the flow has yet to be determined). An equilibrium point is stable if and only if W^u is absent and the flow on W^c has a stable equilibrium at the origin. Even though the center manifold may not be unique, the flows on all possible center manifolds are (topologically) equivalent in a sense to be defined below.

Example 2: A simple example often used to exhibit the nonuniqueness of the center manifold is

$$\begin{aligned} \dot{x}_1 &= x_1^2 \\ \dot{x}_2 &= -x_2 \end{aligned}$$

which has solutions: $x_1(t) = x_1(0)/(1 - tx_1(0))$, and $x_2(t) = x_2(0)e^{-t}$. Combining these, we get

$$x_2(x_1) = [x_2(0)e^{-1/x_1(0)}]e^{1/x_1}$$

which allows us to plot the state trajectories as shown in Fig. 3. Note that (0, 0) is an equilibrium point with

$$A = \begin{bmatrix} 0 & 0 \\ 0 & -1 \end{bmatrix}, \quad E^s = \operatorname{span}\left\{\begin{matrix} 0 \\ 1 \end{matrix}\right\}, \quad E^c = \operatorname{span}\left\{\begin{matrix} 1 \\ 0 \end{matrix}\right\}.$$

Let us consider how to compute the center manifold and the flow on it. It is always possible to separate out the linear part of right hand side of (11) and apply a linear coordinate transformation so that (11) is of the form

$$\begin{aligned} \dot{x}_1 &= Bx_1 + f(x_1, x_2) \\ \dot{x}_2 &= Cx_2 + g(x_1, x_2) \end{aligned}$$

[7] ϕ has continuous derivatives up to order k.

[8] Recall that a manifold is invariant with respect to the flow of a differential equation if any trajectory beginning in the manifold remains in it.

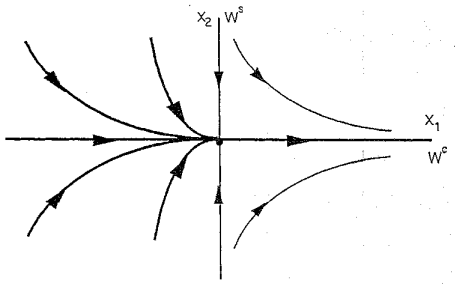

Fig. 3. Notice that the center manifold can be defined using any trajectory beginning with $x_1 < 0$ and joining with it the positive x_1-axis. Also, the center manifold can be chosen to be the entire x_1-axis. This is the only choice which yields an analytic center manifold.

where

- $x_1 \in R^{n_1}, x_2 \in R^{n_2}$,
- f, g and their gradients vanish at the origin,
- the eigenvalues of B have zero real parts, those of C nonzero real parts.

In these coordinates

$$E^c = \operatorname{span}\left\{\begin{matrix} I_{n_1} \\ 0_{n_2 \times n_1} \end{matrix}\right\}.$$

The center manifold is tangent to E^c so that it has a local graph, $x_2 = h(x_1)$, i.e.,

$$\begin{aligned} W^c &= \{x = (x_1, x_2) \in R^n \mid x_2 = h(x_1)\} \\ h(0) &= 0, \partial h(0)/\partial x_1 = 0. \end{aligned}$$

To compute h, observe that

$$\dot{x}_2 = \frac{\partial h(x_1)}{\partial x_1}\dot{x}_1$$

so that using the equations we obtain a partial differential equation

$$Ch(x_1) + g(x_1, h(x_1)) = \frac{\partial h(x_1)}{\partial x_1}[Bx_1 + f(x_1, h(x_1))]$$

which is to be solved for $h(x_1)$ along with the boundary conditions: $h(0) = 0$, $\partial h(0)/\partial x_1 = 0$. Since only a solution near the equilibrium point is needed, one is generally obtained using a power series expansion in x_1. Some simple examples are given in [36]. Once h is obtained, the projection of the center manifold flow onto the x_1 coordinates is

$$\dot{x}_1 = Bx_1 + f(x_1, h(x_1)).$$

C. Bifurcation of Flows Near Equilibria

Perhaps the most important factor contributing to improved understanding of nonlinear phenomenon is the simple notion that it is far more profitable to study families of nonlinear systems rather than individual nonlinear systems. It is the differences in behavior that exist between members

of a family that is most revealing. For instance, the detailed investigation of a system containing a limit cycle is not nearly so informative as the study of a family that contains the system and that exhibits the birth and extinction of the limit cycle.

1) Equivalence of Flows and Structural Stability: A model of a power system, such as (1), is at best an approximation and there is always a concern that conclusions drawn from it may not be consistent with reality. One basic question that should be asked is how sensitive are the predictions of the model to small perturbations of it? We are particularly interested in qualitative properties of the system—namely stability—hence it is essential to know whether qualitative features of the flow change under perturbations of the model. Thus the classical definition of equivalence of flows is appropriate [19], [21], [34].

Definition 2: Two flows φ_t and ψ_t are said to topologically equivalent if there exists a homeomorphism (a continuous map with continuous inverse) taking trajectories of φ_t into trajectories of ψ_t preserving their time orientation.

Roughly speaking, this implies that one flow can be transformed to the other by a continuous deformation of the state space.

Let U be a bounded open set in R^{n+m} and suppose $\mathbf{F}(U)$ denotes the set of all smooth (C^1) maps $F: U \to R^{n+m}$ defined on U. The magnitude of any map $F \in \mathbf{F}(U)$ is taken to be its C^1-norm, i.e.,

$$\|F\| = \sup_{\xi \in U} \left\{ \sum_{i=1}^{n+m} |F_i| + \sum_{i,j=1}^{n+m} \left| \frac{\partial F_i}{\partial \xi_j} \right| \right\}. \tag{12}$$

An *ε-neigborhood* of F in $\mathbf{F}(U)$ is

$$\mathcal{N}_\varepsilon(F) = \{G \in \mathbf{F}(U) \mid \|G - F\| < \varepsilon\}. \tag{13}$$

The magnitude of a DAE or a neigborhood of a DAE can be characterized by identifying F with $\{f, g\}$.

Definition 3: Let $\{f, g\} \in \mathbf{F}(U)$ have an equilibrium point at $(x^*, y^*) \in M$, then $\{f, g\}$ *is locally structurally stable* at (x^*, y^*) if there is a neighborhood $\mathcal{U}$ of (x^*, y^*) in M and an $\varepsilon > 0$ such that for every $\{\tilde{f}, \tilde{g}\} \in \mathcal{N}_\varepsilon(\{f, g\})$ there is a corresponding neighborhood $\tilde{\mathcal{U}}$ of $(\tilde{x}^*, \tilde{y}^*) \in M$ such that the flows $\varphi_t \mid \mathcal{U}$ and $\tilde{\varphi}_t \mid \tilde{\mathcal{U}}$ are topologically equivalent (locally topologically equivalent.)

The main results of interest here regarding structural stability are summarized in the following proposition.

Proposition 1: Suppose the DAE $\{f, g\}$ has an equilibrium point at $(x^*, y^*) \in M$, then $\{f, g\}$ is locally structurally stable at (x^*, y^*) if and only if the equilibrium point is causal and hyperbolic.

Remarks on Proof: Sufficiency is very straightforward because the fact that the system is causal at (x^*, y^*) implies that there is a local representation of the dynamics as an ordinary differential equation and hence standard results apply based on the Hartman–Grobman theorem [21], [34]. The only additional requirement to establish necessity is to verify that a noncausal equilibrium point is not structurally stable. But this is clearly true in view of Theorem 2 in [18].

2) Bifurcation Points: A p-parameter family of DAE's is a C^k, $k \geq 1$, map ϕ: $\mathcal{P} \subseteq R^p \to \mathbf{F}(U)$. Here $\mathcal{P}$ represents a parameter space and we tacitly assume that $\phi(\mathcal{P})$ is a p-dimensional submanifold of $\mathbf{F}(U)$. We denote a family of DAE's by $\{f(\mu), g(\mu)\}$, where $\mu \in \mathcal{P}$ is the parameter. Our goal is to characterize the changes in qualitative behavior that occur in a family $\{f(\mu), g(\mu)\}$ when its parameters are varied. But as we have seen above, a small change from a given parameter value μ_0 can induce a behavioral change only if the system $\{f(\mu_0), g(\mu_0)\}$ is structurally unstable. Hence we have the following definition of a (local) bifurcation point [21], [37].

Definition 4: A value μ_0 for which the flow $\{f(\mu), g(\mu)\}$ is not locally structurally stable near an equilibrium point (x_0^*, y_0^*) of $\{f(\mu_0), g(\mu_0)\}$ is a bifurcation value of μ. The pair, $\mu_0, \{f(\mu_0), g(\mu_0)\}$, is called a bifurcation point.

This definition of a bifurcation point in a given family $\{f(\mu), g(\mu)\}$ has a deficiency in that the family may include a structurally unstable member, but may not exhibit any distinctive behavior. For example, the trivial system $\{f = 0, y - \mu = 0\}, x, y, \mu \in R$, defines a flow that is structurally unstable and unchanged for all values of m. A common alternative definition is [34]: the family has a bifurcation point at $\mu = \mu_0$ if in every neighborhood of μ_0 there are family members that exhibit topologically different behavior. While this definition ensures the existence of dissimilar behaviors near bifurcation points, it suffers annoying technicalities that arise from the fact that while all bifurcation points are structurally unstable, not every structurally unstable point is a bifurcation point. Moreover, the essential difficulty is not really eliminated, just postponed. The remedy is to introduce the concept of a generic family.

3) Genericity: Given a well defined set $\mathcal{G}$ of mathematical objects, such as a set of algebraic equations, vector fields, or DAE's, it is useful to identify properties that are common to virtually all elements in the given set. Such properties are called *generic properties*. Formally, a property is said to be generic if it is shared by a *residual subset* (a countable intersection of open dense sets) [19] of the set $\mathcal{G}$. The elements in $\mathcal{G}$ which exhibit a generic property (the generic points) form an open set in $\mathcal{G}$, and typically the nongeneric points lie on submanifolds of $\mathcal{G}$ with codimension ≥ 1. In some contexts structural stabilty is a generic property in which case structurally unstable elements are referred to as nongeneric.

When examining an arbitrarily selected individual object from $\mathcal{G}$ one expects to observe only generic properties. However, in applications it is often necessary to consider a collection or family of objects within which individual members that do exhibit nongeneric properties are encountered. It is useful to distinguish between those nongeneric behaviors that are likely to be found in families and those that are not. A p-parameter family in $\mathcal{G}$ is a C^1 map s: $\mathcal{P} \subseteq R^p \to \mathcal{G}$. Here we again assume that s$(\mathcal{P})$ is a p-dimensional submanifold of $\mathcal{G}$. The family s contains

nongeneric points if it intersects a manifold $\mathcal{A}$ of nongeneric points. If the intersection of $\mathbf{s}(\mathcal{P})$ and $\mathcal{A}$ is transverse then the intersection is stable in the sense that small changes in the family do not eliminate it. We can say that these nongeneric points contained in $\mathbf{s}(\mathcal{P})$ persist or are nonremovable under perturbations.

In many important cases it is possible to prove that the set of p-parameter families that are transverse to a given submanifold $\mathcal{A}$ of $\mathcal{P}$ form a residual set (in the set of all p-parameter families). Theorems of this type, called 'transversality theorems,' are important in bifurcation analysis. Transversality concepts are discussed at length in [31], [38], [39], [40]. The important implication is that it makes sense to speak of 'generic families' relative to a generic property of interest. This is particularly useful when structural stability is a generic property. In this case, generic families that contain structurally unstable members (bifurcation points) have the property that such members remain even when the family is perturbed. By focusing on bifurcations contained in generic families, we avoid having to deal with special cases that can be eliminated by a small change in the family. Roughly speaking, the main result of significance to us is that generic p-parameter families contain bifurcation points of codimension p or less.

4) Normal Forms: A normal form is a convenient way of representing a class of equivalent systems. It is a member of the class which is 'simple' in some convenient and acceptable sense. Unlike a canonical form, the normal form is not chosen to meet any specific criteria; but the general idea is that it should clearly exhibit the essential features of the system. In view of the Hartman–Grobman theorem, the local behavior of a nonlinear vector field at a hyperbolic equilibrium point is completely described by its linearization. Indeed there is a transformation of coordinates which establishes the equivalence. Hence we need only look at the linearization to determine whether two such nonlinear systems have similar behavior. The linear dynamics (or perhaps its Jordan form) represent a normal form for comparing local dynamics. But behavior near a hyperbolic equilibrium is not particularly interesting because it is not sensitive to perturbations. We need to establish normal forms of vector fields for nonhyperbolic equilibria.[9]

The basic idea is to seek a transformation of coordinates that brings the given vector field into an 'almost' linear form leaving only the nonlinear terms that are not removable by any smooth transformation. These nonlinear terms are essential to the local behavior. An algorithm for reduction to normal form and examples can be found in [21], [34]. We state the basic result following some necessary definitions.

Definition 5: Let $L = Ax$ be linear vector field on R^n. Then we define $H_k :=$ the linear space of vector fields whose components are homogeneous polynomials of degree k, and ad_L: $H_k \to H_k$ is a map defined by

$$ad_L(Y) := [L, Y] = \frac{\partial Y}{\partial x} L - \frac{\partial L}{\partial x} Y, Y \in H_k.$$

Theorem 3 (Normal Form Reduction Theorem): Let $\dot{x} = \phi(x)$ be a smooth system of differential equations with $\phi(0) = 0$ and $L := D_x\phi(0)x$. Choose a complement G_k for $ad_L(H_k)$ in H_k, so that $H_k = ad_L(H_k) + G_k$. Then there is an analytic change of coordinates in a neighborhood of the origin which transforms the system to

$$\dot{y} = Ax + g^2(y) + \cdots + g^r(y) + o(|y|^r)$$

with

$$A := D_x\phi(0) \text{ and } g^k \in G_k, \quad 2 \le k \le r.$$

Proof: A constructive proof is given in [21]. □

Some examples of normal forms are given in Tables 1 and 2.

5) Deformations and Unfoldings: Versal unfoldings provide an efficient characterization of all behaviors exhibited by systems in the vicinity of a system that is locally structurally unstable near an equilibrium point. The following summary follows [31], [34].

Consider the smooth DAE $\{f, g\}$ defined in some neighborhood of $(x^*, y^*) \in R^n \times R^m$. For convenience, we will take $(x^*, y^*) = (0, 0)$. Any family $\{f(\mu), g(\mu)\}$, locally defined at $(x, y, \mu) = (0, 0, 0)$ in $R^n \times R^m \times R^p$, with $\{f_0, g_0\} = \{f, g\}$, is said to be a *deformation* of $\{f, g\}$. Two deformations of $\{f, g\}, \{f(\mu), g(\mu)\}$ and $\{\tilde{f}(\mu), \tilde{g}(\mu)\}$, are *equivalent* if there is a continuous transformation of coordinates $h : \mathcal{N} \subseteq R^n \times R^m \times R^p \to R^n \times R^m, \mathcal{N}$, a neighborhood of (0,0,0), with $h(0, 0, 0) = 0$, such that for each μ, h is a homeomorphism that exhibits the topological equivalence of their flows. A deformation $\{\tilde{f}(\mu), \tilde{g}(\mu)\}$ defined on $R^n \times R^m \times R^p$ is *induced* by a deformation $\{f(\gamma), g(\gamma)\}$ on $R^n \times R^m \times R^q$ if there is a continuous change of parameters h: $R^q \to R^p, \gamma = h(\mu)$, with $0 = h(0)$, such that $\{\tilde{f}(\mu), \tilde{g}(\mu)\} = \{f(h(\mu)), g(h(\mu))\}$. A deformation $\{f(\gamma), g(\gamma)\}$ with q parameters is *versal* if every other deformation is equivalent to one induced by it, and *miniversal* (sometimes called *universal* [41]) if q is the smallest number of parameters needed to define a versal deformation.

If $\{f, g\}$ is structurally unstable, then a deformation of it is said to "unfold the singularity" and a deformation

Table 1 Codimension 1 Bifurcations of Vector Fields

Name	Normal Form/Versal Unfolding
Saddle–Node [21]	$\dot{x} = -x^2 + O(\lvert x\rvert^3) \Rightarrow \dot{x} = \mu - x^2 + O(\lvert x\rvert^3)$
Hopf [21, 34]	$\dot{x} = \begin{bmatrix} 0 & -\omega \\ \omega & 0 \end{bmatrix} x + (x_1^2 + x_2^2)\left\{a_i \begin{bmatrix} x_1 \\ x_2 \end{bmatrix} + b_i \begin{bmatrix} -x_1 \\ x_2 \end{bmatrix}\right\} + O(\lvert x\rvert^5),\ \omega > 0,\ a_i \neq 0$ $\dot{x} = \begin{bmatrix} \mu & -\omega \\ \omega & \mu \end{bmatrix} x + (x_1^2 + x_2^2)\left\{a_i \begin{bmatrix} x_1 \\ x_2 \end{bmatrix} + b_i \begin{bmatrix} -x_1 \\ x_2 \end{bmatrix}\right\} + O(\lvert x\rvert^5)$ or, in polar coordinates $\dot{r} = ar^3 \quad \dot{r} = \mu r + ar^3$ $\dot{\theta} = \omega + br^2 \Rightarrow \dot{\theta} = \omega + br^2$

[9] We confine our discussion of normal forms to vector fields which, for DAE's, means normal forms near causal equilibria. There is, however, an emerging theory for constrained differential equations [23].

Table 2 Codimension 2 Bifurcations of Vector Fields

Name	Normal Form/Versal Unfolding
Cusp, $\mathbb{R}$	$\dot{x} = -x^3 + O(\|x\|^4) \Rightarrow \dot{x} = \mu_0 + \mu_1 x - x^3 + O(\|x\|^4)$
Cusp, $\mathbb{R}^2$ (or double zero) [21, 34]	$\dot{x} = \begin{bmatrix} 0 & 1 \\ 0 & 0 \end{bmatrix} x + \begin{bmatrix} a \\ b \end{bmatrix} x_1^2 + O(\|x\|^3),\ a \neq 0,\ b \neq 0$ $\dot{x} = \begin{bmatrix} 0 \\ \mu_1 \end{bmatrix} + \begin{bmatrix} \mu_2 & 1 \\ 0 & 0 \end{bmatrix} x + \begin{bmatrix} a \\ b \end{bmatrix} x_1^2 + O(\|x\|^3)$
Generalized Hopf (degenerate Hopf) [21, 34, 41]	$\dot{x} = \begin{bmatrix} 0 & -1 \\ 1 & 0 \end{bmatrix} x + a(x_1^2 + x_2^2)^2 \begin{bmatrix} x_1 \\ x_2 \end{bmatrix},\ a \neq 0$ $\dot{x} = \begin{bmatrix} \mu_0 & -1 \\ 1 & \mu_0 \end{bmatrix} x + \mu_1 (x_1^2 + x_2^2) x + a(x_1^2 + x_2^2)^2 \begin{bmatrix} x_1 \\ x_2 \end{bmatrix}$ or, in polar coordinates $\dot{r} = ar^5 + O(r^7)$, $\dot{\theta} = 1$ $\Rightarrow$ $\dot{r} = \mu_0 r + \mu_1 r^3 + ar^5 + O(r^7)$, $\dot{\theta} = 1$
Imaginary pair & zero [21]	$\dot{x} = \begin{bmatrix} 0 & -\omega & 0 \\ \omega & 0 & 0 \\ 0 & 0 & 0 \end{bmatrix} x + \Rightarrow \dot{x} = \begin{bmatrix} 0 \\ 0 \\ \mu_2 \end{bmatrix} + \begin{bmatrix} \mu_1 & -\omega & 0 \\ \omega & \mu_1 & 0 \\ 0 & 0 & 0 \end{bmatrix} x +$ or, in cylindrical coordinates $(a_1, b_1, b_2, b_2 - a_1 \neq 0)$ $\dot{r} = a_1 rz$ $\quad$ $\dot{r} = \mu_1 r + arz$ $\dot{z} = b_1 r^2 + b_2 z^2 \Rightarrow \dot{z} = \mu_2 + b_1 r^2 + b_2 z^2$ $\dot{\theta} = \omega$ $\quad$ $\dot{\theta} = \omega$
Two nonresonant imaginary pairs [21]	$\dot{x} = \begin{bmatrix} 0 & -\omega_1 & 0 & 0 \\ \omega_1 & 0 & 0 & 0 \\ 0 & 0 & 0 & -\omega_2 \\ 0 & 0 & \omega_2 & 0 \end{bmatrix} x + \Rightarrow \dot{x} = \begin{bmatrix} \mu_1 & -\omega_1 & 0 & 0 \\ \omega_1 & \mu_1 & 0 & 0 \\ 0 & 0 & \mu_2 & -\omega_2 \\ 0 & 0 & \omega_2 & \mu_2 \end{bmatrix} x +$ in polar coordinates $(a_{ij} \neq 0, a_{11}a_{22} - a_{12}a_{21} \neq 0;\ m\omega_1 + n\omega_2 \neq 0, \|m\| + \|n\| \leq 4)$ $\dot{r}_1 = a_{11} r_1^3 + a_{12} r_1 r_2^2 + O(\|r\|^5)$ $\quad$ $\dot{r}_1 = \mu_1 r_1 + a_{11} r_1^3 + a_{12} r_1 r_2^2 + O(\|r\|^5)$ $\dot{r}_2 = a_{21} r_1^2 r_2 + a_{22} r_2^3 + O(\|r\|^5)$ $\quad$ $\dot{r}_2 = \mu_2 r_2 + a_{21} r_1^2 r_2 + a_{22} r_2^3 + O(\|r\|^5)$ $\dot{\theta}_1 = \omega_1 + O(\|r\|^2)$ $\Rightarrow$ $\dot{\theta}_1 = \omega_1 + O(\|r\|^2)$ $\dot{\theta}_2 = \omega_2 + O(\|r\|^2)$ $\quad$ $\dot{\theta}_2 = \omega_2 + O(\|r\|^2)$

is often refered to as an *unfolding*. Versal deformations or unfoldings are important because they reveal all possible behaviors which might be observed in perturbations of $\{f, g\}$. Miniversal unfoldings are especially significant because they do this with a minimum number of parameters. The dimension of the γ-space (q) is a measure of the *degeneracy* of the singularity. It follows from analysis of the minversal unfolding $\{f(\gamma), g(\gamma)\}$, that there exists a neighborhood of 0 in γ-space (R^q) which is divided into open regions by surfaces of codimension 1 such that throughout each region $\{f(\gamma), g(\gamma)\}$ exhibits equivalent behavior. The surfaces across which the behavior changes are called *bifurcation surfaces*. These bifurcation surfaces can intersect thereby defining (bifurcation) surfaces of higher codimension. The origin lies at an intersection of codimension q. We refer to this as a singularity of codimension q.

6) Deformations and Unfoldings in Other Contexts: The concept of deformation, described above for DAE's, is frequently applied to other mathematical objects. It is only necessary that it makes sense to speak of parameter dependent families of those objects and to have an appropriate concept of equivalence. For example, in addition to DAE's and vector fields, we note the following:

- Algebraic equations (the study of zeros of equations $f = 0$ under perturbations [37], [41]): Two deformations of a map f: $R^n \rightarrow R^n$, $f(\bullet, \mu)$ and $\tilde{f}(\bullet, \mu)$ are *equivalent* (locally at (0, 0)) if there exists a continuous, near-identity transformation of coordinates $x = h(y, \mu)$ defined on a neighborhood of $(y, \mu) = (0, 0)$, and a continuous, invertible matrix $S(y, \mu)$ such that $f(y, \mu) = S(y, \mu)\tilde{f}(h(y, \mu), \mu)$. Since S is invertible, the zeros of $f(\bullet, \mu)$ correspond to those of $\tilde{f}(\bullet, \mu)$ (in the domain of definition of h). Because of the relevence of this topic to the study of the solution structure of load flow equations, we will discuss the bifurcation of algebraic equations in some detail below.
- Matrices (the study of Jordan forms of matrices under perturbations [31]): Two deformations of an $n \times n$ matrix A, A_μ, and $\tilde{A}_\mu$ are equivalent if they are related by a near-identity similarity transformation, itself dependent on the same parameters, $T(\mu)$ with $T(0) = I$.

Table 3 Bifurcations of Algebraic Equations (Up to Codimension 4) [41]

Name	Codim	Normal Form	Unfolding
Fold (saddle-node) [40, 41, 44]	1	x^2	$x^2+\mu_1$
Cusp [40, 41, 44]	2	x^3	$x^3+\mu_1+\mu_2 x$
Swallowtail [40, 41, 44]	3	x^4	$x^4+\mu_1+\mu_2 x+\mu_3 x^2$
Butterfly [40, 41, 44]	4	x^5	$x^5+\mu_1+\mu_2 x+\mu_3 x^2+\mu_4 x^3$
Hilltop [41]	4	$\begin{bmatrix} x^2-y^2 \\ 2xy \end{bmatrix}$	$\begin{bmatrix} x^2-y^2+\mu_1+\mu_2 x+\mu_3 y \\ 2xy+\mu_4 \end{bmatrix}$
Hilltop [41]	4	$\begin{bmatrix} x^2 \\ y^2 \end{bmatrix}$	$\begin{bmatrix} x^2+\mu_1+\mu_2 y \\ y^2+\mu_3+\mu_4 x \end{bmatrix}$

- Pencils (the study of the zero structure of linear systems under perturbations [42]): Two deformations of an $n \times m$ pencil $sA + B, sA_\mu + B_\mu$ and $s\tilde{A}_\mu + \tilde{B}_\mu$ are equivalent if they are related by a near identity, strict equivalence transformation [43], i.e., $sA_\mu + B_\mu = P(\mu)[s\tilde{A}_\mu + \tilde{B}_\mu]Q^{-1}(\mu)$ with $P(0) = I$ and $Q(0) = I$.

D. The Generic Bifurcations

In Tables 1 and 2 we summarize the generic codimension 1 and codimension 2 bifurcations of vector fields from an equilibrium point, that is, the local bifurcations that will be found in one and two parameter generic families. The normal form and a versal unfolding is given in each case. We can not describe herein all of the behavior exhibited by these bifurcations, but references which do so are given.

Similarly, in Table 3 we summarize the bifurcations of algebraic equations (called singularities) up to codimension 4. Bifurcations of algebraic equations are important to us because it is often useful to study the equilibrium point structure, and parametrically induced changes to it, separately from, or as an adjunct to, considering dynamical issues (vector field properties). Notice that the bifurcations of codimension less than 4 in Table 3 involve only one independent variable, whereas bifurcations of codimension 4 may involve two. Singularities involving two or more independent variables have not been completely classified [37, Chap. 7], [41, Chap. 9]. It is also useful to note that any singularity involving a single independent variable directly corresponds to a 'catastrophe' which gives some additional interpretations [40], [44].

Example 3: (The Saddle-Node Bifurcation): In this example we give an illustration of the phase portrait variations associated with a saddle-node bifurcation. Consider the 2-D system

$$\dot{x}_1 = x_1^2 + \mu$$
$$\dot{x}_2 = -x_2$$

Three different state space diagrams are illustrated in Fig. 4 showing the prebifurcation, critical, and postbifurcation cases. Notice that two equilibria, one stable the other unstable, merge into a single semistable equilibrium and then the equilibrium point vanishes as the parameter μ changes from a negative to a positive number.

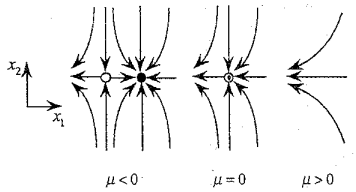

Fig. 4. Phase portraits associated with saddle-node bifurcation.

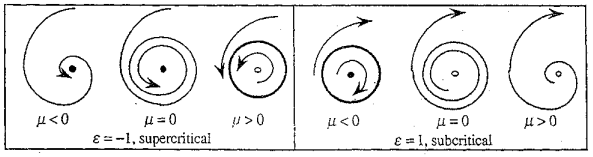

Fig. 5. State space trajectories for the supercritical and subcritical Hopf bifurcations.

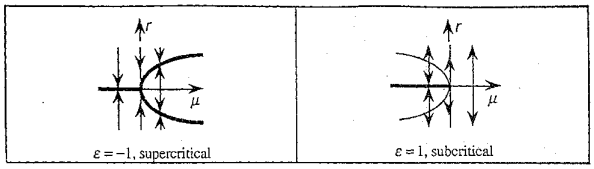

Fig. 6. Bifurcation diagrams for the supercritical and subcritical Hopf bifurcations. $r = 0$ corresponds to the equilibrium point. Stable equilibria and orbits are indicated by bold curves.

Example 4: (The Hopf Bifurcation): Consider the system

$$\begin{bmatrix} \dot{x}_1 \\ \dot{x}_2 \end{bmatrix} = \begin{bmatrix} \mu & -1 \\ 1 & \mu \end{bmatrix} \begin{bmatrix} x_1 \\ x_2 \end{bmatrix} + (x_1^2 + x_2^2) \left\{ \varepsilon \begin{bmatrix} x_1 \\ x_2 \end{bmatrix} + \begin{bmatrix} -x_2 \\ x_1 \end{bmatrix} \right\}$$

or, equivalently, in polar coordinates ($x_1 = r\sin\theta, x_2 = r\cos\theta$)

$$\dot{r} = r(\mu + \varepsilon r^2), \quad \dot{\theta} = 1 + r^2.$$

We will consider two cases, $\varepsilon = \pm 1$. μ is the adjustable parameter. The state space trajectories are illustrated in Fig. 5. Let us consider the the supercritical ($\varepsilon = -1$) case first. For $\mu < 0$ there is a hyperbolic, stable equilibrium point at the origin. When $\mu = 0$, the equilibrium point at the origin is no longer hyperbolic, it has a 2-D center manifold with a pair of imaginary eigenvalues $\pm i$. The equilibrium point of the (nonlinear) system is, however, asymptotically stable although not exponentially stable. When $\mu > 0$, the origin is again hyperbolic, but it is unstable and there exists a stable periodic orbit with constant radius $r = \mu^{1/2}$.

Another pictorial view of the Hopf bifurcation is provided by the bifurcation diagrams of Fig. 6. The oscillation amplitude r is plotted versus the parameter μ. Here we again see that in the supercritical case, the stable equilibrium becomes unstable as μ changes from negative to positive and a stable periodic trajectory emerges. In the subcritical case the periodic trajectory is unstable and exists for negative values of μ. For applications this is a crucial distinction. In the supercritical case, even though the origin is unstable after bifurcation, trajectories are still attracted into its vicinity

if the oscillation amplitude is small. The subcritical case can be very dangerous because the unstable limit cycle bounds the domain of attraction of the stable origin and this domain shrinks as the bifurcation point is approached from the left.

III. Computations and Examples

When investigating bifurcations in power systems we want to acomplish three things: 1) locate bifurcation points, 2) characterize the associated behavior, and 3) identify remedial actions. Our basic strategy is as follows: Suppose a power system is operating in a stable equilibrium state corresponding to a particular parameter value. In order to ensure continued, reliable operation, we seek to identify nearby bifurcation points since points of incipient instability are always bifurcation points. The term 'nearby' can assume different meanings, but we intend it to mean that the bifurcation parameter value is close to the parameter value of the current operating state. The choice of parameter set can be especially important to the practical significance of this measure. Some parameters may be uncontrollable (such as load parameters) while others may be controllable (such as generation distribution parameters or tap positions). In such a context we can try to find the closest bifurcation point. Once having located a bifurcation point it is necessary to identify the kind of behavior that is associated with it—some may be more dangerous than others. This can be accomplished by computing enough information to identify its normal form, after which one consults a finite, pre-established catalog. Recognizing that the bifurcation point lies in a set of points which form a boundary in the parameter space, we seek to characterize the boundary so as to identify remedial changes of controllable parameters if necessary.

It is useful to distinguish between the study of bifurcations of the equilibrium equations (static bifurcation analysis) and the study of bifurcations of vector fields (*dynamic* bifurcation analysis). Clearly, since the equilibrium equations identify equilibrium (or fixed) points of the associated vector fields, static bifurcation is always associated with dynamic bifurcation. In addition to the implications that static bifurcation has with regard to dynamics, static bifurcations are of interest in their own right because in load flow analysis questions about existence and number of equilibria are significant. Static bifurcation analysis is a far simpler problem than dynamic bifurcation analysis and the analytical technology is more mature.

Local bifurcations of the vector fields that accompany DAE descriptions of power systems are associated with equilibria that are either noncausal or nonhyperbolic. When a causal, nonhyperbolic equilibrium point has a simple eigenvalue at the origin and no other eigenvalues on the imaginary axis all necessary information[10] can be obtained from static bifurcation analysis based on the Lyapunov–Schmidt reduction. If it has only a pair of simple complex eigenvalues on the imaginary axis, the associated generic bifurcations (the Hopf and generalized Hopf bifurcations) are dynamic but they can be investigated using essentially the same tools as static bifurcations. Other, more complex situations, require a fundamentaly dynamic treatment based on center manifold theory. In the following paragraphs we will describe tools for locating and classifying static and generalized Hopf bifurcations. While we will not specifically address locating noncausal points, the method we describe for static bifurcation can be modified to find noncausal points.

A. Static Bifurcation

In this section, we consider bifurcation of the load flow (3). For convenience, we collect the dependent variables x and y into a single vector which we denote x. This admittedly abusive notation will not lead to confusion because there is no reason to distinguish between these variables in the following discussion. Similarly, collect the pair of functions f and g into the single function F: $R^n \times R^p \rightarrow R^N$, $N = n + m$, so that (3) can be rewritten as $F(x, \mu) = 0$. We seek to investigate the zeros of F (equilibria) as a function of the parameter vector μ.

Conventional numerical methods for computing equilibria, such as the Newton–Raphson method, must be modified in order to obtain reliable results near bifurcation points.[11] Two methods have been applied to power system analysis: the continuation (or homotopy) method [46] and the direct (or point of collapse) method [47]. The direct method proposed by Seydel [47] to compute the branch points in single-parameter nonlinear algebraic equations has proved remarkably effective in power system applications. Many investigators have implemented variants of this approach, imaginatively tailored to the special features and requirements of power systems [48]–[51]. We refer to these as a group as the Newton–Raphson–Seydel method. The continuation method has also been applied to power systems [52]–[56]. Cañizares and Alvarado [55] compare performance of the two methods for a variety of large power systems.

In the following, we summarize both the direct method and the continuation method for single parameter problems and their application to power systems. Then we show how the direct method can be extended to find static bifurcation points in multiparameter power systems. When this method is combined with the Lyapunov–Schmidt reduction we not only obtain reliable determination of equilibria but also a complete classification of the local equilibrium point structure.

1) Locating Static Bifurcation Points: The Single Parameter Case—Direct Method: The Newton–Raphson method breaks down near (static) bifurcation points, i.e., when F_x is singular ($\mathrm{rank}[F_x] < N$). In generic one-parameter families the dimension of $\mathrm{Ker}[F_x]$ at a bifurcation point is precisely one ($\mathrm{rank}[F_x] = N - 1$). Thus to locate such a

[10] This includes local characterization of the bifurcation sets, and the number of equilibria and their stability under small perturbations.

[11] Dynamic simulation near static bifurcation points is also a challenge [45].

point we seek values for $x \in R^N, \mu \in R^1$ and nontrivial v or $w \in R^N$ which satisfy

$$F(x,\mu) = 0 \tag{14a}$$
$$F_x(x_i,\mu)v = 0 \quad \text{or} \quad w^T F_x(x_i,\mu) = 0. \tag{14b}$$

The requirement of nontriviality of v, w may be stated

$$\|v\| = 1 \quad \text{or} \quad \|w\| = 1. \tag{14c}$$

The solution set $\mathcal{E} = \{(x,\mu) \in R^{\mathcal{N}+1} \mid F(x,\mu) = 0\}$ is a regular imbedded submanifold of dimension one in $R^{\mathcal{N}+1}$ if and only if $\text{rank}[F_x F_\mu] = N$ on $\mathcal{E}$. If this is the case, then the requirement that v, w be nontrivial can be reformulated

$$F_\mu(x,\mu)v = 1 \quad \text{or} \quad w^T F_\mu(x,\mu) = 1. \tag{14d}$$

One basic approach to finding bifurcation points is to apply the Newton–Raphson method to (14). This is the basic Newton–Raphson–Seydel method. Data that satisfies (14) will be denoted x_b, μ_b, v_b, w_b and we designate the Jacobian $J_b := F_x(x_b, \mu_b)$. Note that the vectors v_b, w_b have special significance. They are, respectively, the right and left eigenvectors corresponding to the zero eigenvalue of J_b. The eigenvector v_b spans the kernel of J_b and w_b spans the kernal of J_b^T. Moreover, v_b identifies those dependent variables that play a role in the bifurcation. That is, only those elements of x that correspond to nonzero entries in v_b will exhibit the bifurcation behavior. w_b will be seen, below, to provide useful information in multiparameter problems [16], [57].

Once a bifurcation point is located, it is feasible to modify the above method to compute points around the fold (nose) of the equilibrium surface

$$\begin{aligned} F(x,\mu) &= 0 \\ [F_x(x,\mu) - \lambda I]v &= 0 \end{aligned} \tag{15}$$

for values of $\lambda \in [-\varepsilon_1, \varepsilon_2]$ with $\varepsilon_1, \varepsilon_2 > 0$.[12] This allows computation of equilibrium points close to the bifurcation point where conventional Newton–Raphson calculations would fail. Of course, $\lambda = 0$ corresponds to the bifurcation point.

The above method can be effective but it has the disadvantage that is significantly more computationally intensive than a standard load flow. It involves solving $2N + 1$ equations as opposed to N, and it requires computing second order derivatives of F. However, since (14b and c) are linear in w and v it is possible to devise potentially more efficient alternatives. An approach suggested in [51] will be briefly summarized. Choose a smooth scalar valued function $h(x)$ and replace μ with the new parameter η according to $\mu = \eta h(x), \eta \in R$. First, multiply (14d) by $\eta h_x^T(x)$ and add the result to (14b) to obtain

$$[F_x(x,\eta h(x)) + \eta h_x^T(x) F_\mu^T(x,\eta h(x))]v = \eta h_x^T(x). \tag{16}$$

It is intended that

$$J_m := [F_x(x,\eta h(x)) + \eta h_x^T(x) F_v^T(x,\eta h(x))]$$

will be nonsingular at solutions of (14) even though $J = D_x F$ must be singular. In this event, (16) determines v. It remains to solve (14a) and (14d) for (x,η). Let us collect (14a, d) and (16) to form

$$F(x,\eta h(x)) = 0 \tag{17a}$$
$$J_m(x,\eta)v = \eta h_x^T(x) \tag{17b}$$
$$F_\mu^T(x,\eta h(x))v = 1. \tag{17c}$$

In principle, we can solve (17b) for $v = J_m^{-1} h_x^T \eta$ so that (17c) can be written

$$(F_\mu^T(x,\eta h(x)) J_m^{-1}(x,\eta) h_x^T(x))\eta = 1.$$

Thus we need solve the remaining equations for (x,η)

$$F(x,\eta h(x)) = 0 \tag{18a}$$
$$a(x,\eta)\eta = 1. \tag{18b}$$

where the scalar function $a(x,\eta)$ is

$$a(x,\eta) := F_\mu^T(x,\eta h(x)) J_m^{-1}(x,\eta) h_x^T(x). \tag{19}$$

One approach to finding solutions to (19) would be to employ a standard Newton–Raphson iteration. To do so requires computation of $\partial a/\partial x$ and $\partial a/\partial \eta$. The standard Newton–Raphson iteration applied to (19) yields

$$\begin{aligned} J_m^k \Delta x^{k+1} + F_\mu^k h(x) \Delta \eta^{k+1} &= -F^k \\ a_x^k \Delta x^{k+1} + [a^k + a_\eta^k \eta^k]\Delta \eta^{k+1} &= -a^k \eta^k + 1. \end{aligned}$$

Because of the presence of $a_x(x,\eta)$ and $a_\eta(x,\eta)$, second derivatives of F are still required. An alternative suggested in [51] is to apply a standard Newton–Raphson iteration with respect to x to (18a) and then solve (18b) for η (in Gauss–Seidel fashion) to obtain

$$\begin{aligned} J_m^i(x_{i+1} - x_i) &= -F(x_i, \eta_i h(x_i)) \\ \eta_{i+1} &= 1/a(x_{i+1}, \eta_i). \end{aligned} \tag{20}$$

In order to discuss the convergence of this method, note that (20) constitute an iteration of the map φ: $R^{N+1} \to R^{N+1}$

$$\varphi(x,\eta) = \begin{bmatrix} x - J_m^{-1}(X,\eta)F(x,\eta h(x)) \\ a(x - J_m^{-1}(x,\eta)F(x,\eta h(x)),\eta)^{-1} \end{bmatrix}. \tag{21}$$

Proposition 2: Suppose x^*, μ^*, v^* satisfies (14), $h(x) \neq 0$ on a neighborhood of $x^*, a(x^*,\eta^*) \neq 0$ and $J_m(x^*,\eta^*)$ is nonsingular where $\eta^* = \mu^*/h(x^*)$. Then the map φ is

[12] The bifurcation point ($\lambda = 0$) data x_b, μ_b, v_b is a regular solution of (15) along with the nontriviality condition for v so that the Implicit Function theorem guaranties the existance of a unique solution $x(\lambda), \mu(\lambda), v(\lambda)$ on a neighborhood of $\lambda = 0$.

well defined on a neighborhood of (x^*, η^*) and (x^*, η^*) is a fixed point of φ. Furthermore, if

$$|\eta^{*2} a_x(x^*, \eta^*) J_m^{-1}(x^*, \eta^*) F_\mu(x^*, \eta^* h(x^*)) h(x^*) - \eta^{*2} a_\eta(x^*, \eta^*)| < 1$$

then φ is a contraction on a neighborhood of (x^*, h^*).

Proof: The first conclusion that (x^*, η^*) is a fixed point is obvious. To show that φ is a contraction on a neighborhood of (x^*, v^*) it is sufficient to show that the spectral radius of $D\varphi(x^*, \eta^*)$ is less than 1. Direct computation leads to

$$D\varphi^* = \begin{bmatrix} \frac{\partial \varphi_1}{\partial x} & \frac{\partial \varphi_1}{\partial \eta} \\ \frac{\partial \varphi_2}{\partial x} & \frac{\partial \varphi_2}{\partial \eta} \end{bmatrix} = \begin{bmatrix} 0 & J_m^{*-1} \\ 0 & \eta^{*2} a_x^* J_m^{*-1} F_\mu^* h^* - \eta^{*2} a_\eta^* \end{bmatrix}.$$

Clearly, all of the eigenvalues of $D\varphi^*$ are zero except one: $\lambda = \eta^{*2} a_x^* J_m^{*-1} F_\mu^* h^* - \eta^{*2} a_\eta^*$. Thus the conclusion follows. □

Remarks:

1) The Proposition simply states that, provided the conditions are satisfied and if initial estimates (x^0, μ^0) are sufficiently close to (x^*, μ^*) the iteration

$$\begin{bmatrix} x^{i+1} \\ h^{i+1} \end{bmatrix} = \varphi(x^i, h^i)$$

will converge to (x^*, η^*). Obviously, we take $\eta^0 = \mu^0 / h(x^0)$.

2) The choice of $h(x)$ is arbitrary except that h must be differentiable, the zeros of h must not coincide with bifurcation values of x, and J_m must be nonsingular at bifurcation points. The last point is the reason for introducing $h(x)$ in the first place. If the manifold $\mathcal{E}$ is regular at (x^*, μ^*) and if $\mu^* \neq 0$ (so that $\eta^* \neq 0$) then almost any vector $hx(x^*)$ results in J_m nonsingular at x^*.

3) In actual computation, one would implement

$$\begin{aligned} J_{m,i}(x_{i+1} - x_i) &= -F(x_i, \eta_i h(x - i)) \\ J_{m,i+1} b_{i+1} &= h_x^T(x_{i+1}) \\ \eta_{i+1} &= 1/(F_\mu(x_{i+1}, \eta_i h(x_{i+1}) b_{i+1}. \end{aligned} \tag{22}$$

Notice that b is just a scaled verson of v hence, it is the null space spanning vector for J. For computational efficiency, especially for large systems, it is a significant advantage to use $J_{m,i}$ rather than $J_{m,i+1}$ in the second equation.

4) The computational experience of Carpaneto *et al.* [51] shows that for several standard power systems, including the IEEE 57-bus system, the application of the iteration of the last remark convergences very quickly.

5) The function $h(x)$ can influence the convergence properties of the algorithm. A specific choice is discussed in [51]. An analogous "regularization" function is typically introduced when continuation methods are applied to load flow calculations near bifurcation points [53], [58].

6) Chiang and Jean-Jumeau [59] have recently reported results using a similar method on a 234-bus power system. In fact, both [51] and [59] consider the (commonly used) special case in which the parameter enters the load flow equation linearly

$$F(x, \mu) = f(x) - \mu b. \tag{23}$$

In this case it is easy to confirm that, with the choice $h(x) = b^T x$, (19) above constitute the $N + 1$ equations solved in [59]. The main difference appears to be that [51] uses the mixed method of (20) to solve (19). whereas [59] successively applies Brent's method (an interval method [60]) to solve (18b) for η and then a Davidon-Fletcher-Powell method (a quasi-Newton method [60], [61]) to solve (18a) for x. Both methods effectively reduce the number of equations solved from the $2N + 1$ equations required by straight forward implementation of the Newton–Raphson–Seydel method to $N + 1$, and neither require computation of second derivatives.

2) The Single Parameter Case: Continuation Method: Continuation methods for the numerical solution of nonlinear problems have been around since at least the 1930's [46], [62], [63]. Applications of continuation methods to power systems are described in [52], [55], [56], [64]. The basic idea of continuation is simple and has many applications. Consider a parameter dependent family of mathematical problems $\mathcal{P}(\mu)$. Suppose the problem $\mathcal{P}(\mu_0)$ is easy to solve, but we wish to find a solution to $\mathcal{P}(\mu^*)$. Then the idea is to sequentially solve a sequence of problems $\mathcal{P}(\mu_i)$, $i = 0, \ldots, K$, terminating with $\mu_K = \mu^*$. Successive solutions are extrapolated to get a starting value for an iterative solution of the next problem.

Let us apply this approach to the one-parameter family (14a). Suppose that a solution (x_0, μ_0) is known, i.e., $F(x_0, \mu_0) = 0$. We wish to find the solution x^* corresponding to the parameter value μ^*. Applying the continuation method, we divide the interval $[\mu_0, \mu^*]$ into a large number K of subintervals and generate successive solutions, x_i, $i = 1, \ldots, K$, as follows. To generate the first solution, we take as a starting value $x_1^0 = x_0$ and then apply Newton's method (for example) to determine x_1. For subsequent starting values, x_i^0, $i > 1$, we could continue the zeroth order extrapolation, i.e.,

$$x_i^0 = x_{i-1} \tag{24a}$$

or we could use a linear extrapolation (called the secant method in [56])

$$x_i^0 = x_{i-1} + (x_{i-1} - x_{i-2}) \frac{\mu_i - \mu_{i-1}}{\mu_{i-1} - \mu_{i-2}} \tag{24b}$$

followed by Newton's method. If one takes this to the extreme so that $K \to \infty$, $\Delta\mu \to 0$, then the successive solutions are connected by the differential equation

$$F_x(x, \mu) dx + F_\mu(x, \mu) d\mu = 0$$

or

$$F_x(x,\mu)\frac{dx}{d\mu} + F_\mu(x,\mu) = 0. \tag{25}$$

In principle, an implicit ordinary differential equation solver can be used, with μ as the independent variable, to obtain the curve $x(\mu)$ for $\mu \in [\mu_0, \mu^*]$.

Obviously, this method must be modified when collapse points exist in the interval $[\mu_0, \mu^*]$ because the Jacobian $F_x(x,\mu)$ is singular at such points. There are a number of ways to remedy this situation. They are based on the fact that a generic one-parameter equation $F(x,\mu) = 0$ has a smooth solution curve in the $N+1$ dimensional (x,μ) space [31]. This means that

$$\begin{aligned}&\operatorname{rank}[F_x(x,\mu) \quad F_\mu(x,\mu)]\\ &\quad = N \text{ on the set } \{(x,\mu) \in R^{N+1} \mid F(x,\mu) = 0\}.\end{aligned}$$

In other words, the matrix $[F_x \quad F_\mu]$ has N linearly independent columns. Consequently, it is always possible to rearrange the variables so that an appropriate state variable plays the role of the independent varable and the parameter is one of the n dependent variables. This is essentially the problem of identifying N linearly independent columns from $[F_x \quad F_\mu]$. When F_x is singular, the highly sensitive states appear as nonzero entries in the null space spanning vector. Any one of these is an appropriate replacement for μ. Cañizares and Alvarado [55] suggest tracking the relative change in system variables (x and μ) and switching to the most sensitive for use as the parameter as the singular point is approached.

An attractive alternative 'blends' the $N+1$ independent columns into N independent columns by the use of a state dependent transformation of parameters $\mu = \eta h(x), \eta \in R$, precisely as was done in deriving (16) above. Thus we seek to find the curve $x(\eta) \subset R^{N+1}$, passing through the point $(x_0, \eta_0) = (X_0, \mu_0/h(x_0))$, and satisfying $F(x, \eta h(x)) = 0$. Then the Jacobian F_x is replaced by

$$[F_x(x,\eta h(x)) + F_\mu(x,\eta h(x))h_x^T(x)]$$

and the differential (25) is replaced by

$$[F_x(x,\eta h(x)) + F_\mu(x,\eta h(x))h_x^T(x)]\frac{dx}{d\eta} + F_\mu h(x) = 0. \tag{26}$$

The solution terminates when $\eta_1 = \mu_1 h(x_1)$. The idea of course is that the matrix $[F_x + F_\mu h_x^T]$ will not be singular on the interval of interest. Continuation methods with this type of 'reglarization' are applied to power systems in [53], [54]. We have already noted the connection between regularization used with the continuation method and the direct method described above.

A third approach, perhaps the most common, for dealing with singularities in F_x is to reparameterize the problem in terms of the arc length s. This is accomplished as follows. First, we treat the parameter μ as a dependent variable. To make this explicit define $\bar{x} = [x^T, \mu]^T$, and $\bar{F}(\bar{x}) := F(x,\mu)$. We seek a curve $\bar{x}(s) \subset R^{N+2}$ that satisfies

$$\bar{F}(\bar{x}(s)) = 0 \tag{27a}$$

and passes through the point $(\bar{x}, s) = ((x_0, \mu_0), 0)$, where s is defined with respect to any convenient local reference point on the curve, $(\bar{x}(s_r), s_r)$, by the relation

$$(s - s_r)^2 = \|\bar{x}(s) - \bar{x}(s_r)\|^2. \tag{27b}$$

Equations (27) may be viewed as $N+1$ equations in $N+1$ unknowns, $\bar{x}$, with a single parameter s. We generate a sequence of solutions $\bar{x}_i$, $i = 1, \ldots, K$, corresponding to a specified sequence s_i, $i = 1, \ldots K$. At each stage, we can generate a starting value for $\bar{x}_i$ using formulas (24)—with x replaced by $\bar{x}$—and then apply an iterative process to (27) with $s = s_i$ and $s_r = s_{i-1}$ in (27b). Specific implementations of this process to power systems are described in [55], [56].

The differential equation approach can also be used with the arc length parameterization. In this case the arc length is defined by the differential equation

$$\left\|\frac{d\bar{x}}{ds}\right\|^2 = 1 \tag{28a}$$

and the differential equation (25) is replaced by

$$\bar{F}_{\bar{x}}\frac{d\bar{x}}{ds} = 0. \tag{28b}$$

The system of $N+1$ differential equations (27a and b) is to be solved for $\bar{x}(s) \subset R^{N+2}$. Note that the special structure of (28) allows reduction to quadratures. Since $\bar{F}_{\bar{x}}(\bar{x})$ has rank N along the solution curve, there is an $N+1$-vector $\gamma(\bar{x})$ whose span is the kernel of $\bar{F}_{\bar{x}}(\bar{x})$ at any point on the curve. γ can be chosen to have unit length. Then (28a and b) are satisfied by solutions of

$$\frac{d\bar{x}}{ds} = \gamma(\bar{x}). \tag{29}$$

To our knowledge, the only application of the differential equation solution method to power systems appearing in the literature is Thomas *et al.* [65], although Chiang *et al.* [56] use an equivalent to (29) to extrapolate a starting estimate for a solution via Newton's method but only for the first step after which they use linear extrapolation.

3) The Multiparameter Case: When the number of parameters is $k = 1, 2, 3$ the generic situation is $\dim(\operatorname{Ker}(D_x F)) = 1$ (see the discussion in [37, Chap. 7], [41, Chap. 9], and Table 3). In the following treatment of the multiparameter case we assume that $\dim(\operatorname{Ker}(D_x F)) = 1$. The strategy is to locate the bifurcation value closest to a given parameter value μ_0. Since coordinates used to define μ may be arbitrarily shifted, we take $\mu_0 = 0$. The problem of locating the closest static bifurcation point in multiparameter power systems has been raised by several investigators including [66]–[71].

Redefine (14a-c) as $\psi(x, v, \mu) = 0$

$$\psi(x, v, \mu) := \begin{bmatrix} F(x, \mu) \\ D_x F(x, \mu) v \\ \|v\| - 1 \end{bmatrix}$$

with $x \in \mathcal{H} \simeq R^{\mathcal{N}}, v \in \mathcal{U} \simeq R^{\mathcal{N}}, \mu \in \mathcal{M} \simeq R^k$. We seek a point (x, v, μ) in $\mathcal{Y} := \mathcal{H} \times \mathcal{U} \times \mathcal{M} \simeq R^{2\mathcal{N}+k}$, such that $\|\mu\|^2$ is minimum with $\psi(x, v, \mu) = 0$. To do so, introduce a Lagrange multiplier l, and construct the Lagrangian function

$$L = \|\mu\|^2 + \lambda^T \psi(x, v, \mu) \qquad \lambda \in R^{2N+1}. \tag{30}$$

Then necessary conditions are

$$\begin{aligned} \frac{\partial L}{\partial \lambda} &= \psi(x, v, \mu) = 0 \\ \frac{\partial L}{\partial x} &= \lambda^T \frac{\partial \psi}{\partial x} = 0 \\ \frac{\partial L}{\partial v} &= \lambda^T \frac{\partial \psi}{\partial v} = 0 \\ \frac{\partial L}{\partial \mu} &= 2\mu^T + \lambda^T \frac{\partial \psi}{\partial \mu} = 0. \end{aligned} \tag{31}$$

We can rewrite the last three equations as

$$\Phi^T \lambda = b \tag{32}$$

where

$$\Phi := \left[\frac{\partial \psi}{\partial x}, \frac{\partial \psi}{\partial v}, \frac{\partial \psi}{\partial \mu}\right], \quad b = [0_{1\times 2N}, -2\mu^T]^T.$$

Now, Let Φ^* denote the right inverse of Φ[13] and obtain from (32)

$$\lambda = \Phi^{*T} b \tag{33a}$$

$$[I - \Phi^* \Phi]^T b = 0. \tag{33b}$$

Notice that $[I - \Phi^*\Phi]$ has only $k-1$ linear independent rows. Having eleminated λ, our problem is now completely characterized by (33b) along with the first of (31). Thus we have increased the dimension of the system from $2N+1$ in the one parameter case to $2N+k$. Points (x, v, μ) that satisfy the enlarged system are the extremal bifurcation points. One way to compute them using numerical iteration is given by the following algorithm. Let the parameter vector μ be expressed $\mu = me$, where m is a scalar and e is a unit vector that specifies a direction in parameter space.

Algorithm

Step 1: Initialize: choose an intial search direction $e_0 \in R^k$; and initial values $x_0 \in R^N, v_0 \in R^N$.

[13]For a generic function $\psi : R^{2N+k} \to R^{2N+1}$, the solution set of $\psi = 0$ is a smooth $k-1$ dimensional (regular) manifold and $\text{rank}[\Phi] = 2N+1$, its maximum rank, on the set [72, Section 31]). Thus for a generic family, Φ^* exists on a neighborhood of any solution of $\psi = 0$.

while $\|e_i - e_{i-1}\| >$ tolerance and $i \le i_{\max}$

Step 2: Solve $\psi(x, v, me_{i-1}) = 0$ for $x_i, v_i, m_i)$; use starting values $(x_{i-1}, v_{i-1}, m_{i-1})$.

Step 3: Update the search direction e_{i-1} to e_i in order to reconcile $[I - \Phi^*\Phi]^T b = 0$.

Step 4: Update i: $i = i + 1$

end

Step 2 is solved using the Newton–Raphson–Seydel method. Step 3 is achieved by using one of the recursions described below.

4) Geometric Interpretation: Consider the set $\mathcal{B} = \{(x, v, \mu) \in \mathcal{H} \times \mathcal{U} \times \mathcal{M}\} \mid \psi(x, v, m = 0\}$ $\mathcal{B}$ is a regular, $k-1$ dimensional submanifold of $\mathcal{Y}$ provided $= \text{rank}[\Phi] = 2N+1$ (full rank) on $\mathcal{B}$. Consider a point $p \in \mathcal{B}$. Then $p + \text{Ker}(\Phi(p))$ is the tangent space to $\mathcal{B}$ at p. Define $\gamma(x, v, \mu) = \|\mu\|^2$ and the family of sets (cylinders) $\mathcal{C}(c) = \{(x, v, \mu) \in \mathcal{H} \times \mathcal{U} \times \mathcal{M}\} \mid \gamma(x, v, m) = c\}$. Each set $\mathcal{C}(c)$ is a regular submanifold of codimension one in $\mathcal{Y}$ provided $\mu \neq 0$. Equations (32) are equivalent to the geometric conditions $b \in \text{Im}(\Phi^T)$ or $\text{Ker}(F) \subseteq \text{Ker}(b^T)$ which simply means that the curve $\mathcal{B}$ is tangent to the cylinder $\mathcal{C}(c)$ at the point of contact. Thus we have the following result.

Proposition 3: Suppose the point $p \in \mathcal{B}$. Then there exists a unique c^* such that $p \in \mathcal{C}(c^*)$. Furthermore, $\|\mu\|^2 = c^*$ is a minimum only if $\text{Ker}\Phi(p)) \subseteq \text{Ker}(b^T(p))$ or, equivalently, $b(p) \in \text{Im}\,\Phi^T(p))$.

Let $\mu = me$, m a real valued scalar and e a unit vector in $\mathcal{M}$. Suppose that a point $p = (x_i, w_i, m_i e_i) \in \mathcal{B}$ has been located by scalar search with respect to m and with e_i fixed. Note that if $\text{Im}\,\Phi^T(p)) \simeq R^{2\mathcal{N}+1}$ and $\mathcal{M} \simeq R^k$ are considered as subspaces of $\mathcal{Y} \simeq R^{2\mathcal{N}+k}$ then their intersection $\mathcal{I}$ is at least (also generically) of dimension one. Furthermore, it is clear that $b(p) \in \text{Im}\,\Phi^T(p))$ if and only if $e_i \in \mathcal{I}$. The natural projection which maps any element of $\mathcal{Y}$ onto $\mathcal{M}$ is $P = [0_{k\times 2n} \quad I_{k\times k}]$. The bifurcation set in the parameter space $\mathcal{M}$ is the projection $\Sigma := P\mathcal{B}$. Even when $\mathcal{B}$ is smooth and regular, Σ is likely not be. Note that the natural projection of $\text{Ker}\,\Phi(p)) \simeq R^{k-1}$ onto $\mathcal{M} \simeq R^k$ generically produces a codimension-one linear surface in $\mathcal{M}$. In fact, this surface is a tangent hyperplane to the bifurcation surface $\Sigma \subset \mathcal{M}$ at $\mu_i = m_i e_i$. In view of these remarks, we suggest the following recursions for implementing step 3 of the algorithm.

Recursion Method 1: If $\mu_i = m_i e_i$ is a regular point of the bifurcation surface Σ, then the condition $\text{Ker}\,\Phi(p)) \subseteq \text{Ker}\,(b^T(p))$ requires that e_i is orthogonal to $\mathcal{T} := P\mathcal{G}$. If it is not, then choose a new direction: e_{i+1} that is so. The constructions may be implemented as follows:

— Let $Q := \Phi^*\Phi$, where Φ^* is a right inverse of ϕ. Then $\text{Ker}\,\Phi(p)) = \text{Ker}\,(Q) = (I - Q)\mathcal{Y}$ and $\mathcal{T} = P\mathcal{G} = P(I - Q)\mathcal{Y}$.

— To obtain e_{i+1} othogonal to $\mathcal{T}$, choose $e_{i+1} \in \text{Ker}\,([I - Q]^T P^T)$. This space is generically of dimension one.

Recursion Method 2: Note that $\mathcal{Y} = \text{Im}\,\Phi^T(p)) \oplus \text{Ker}\,\Phi(p))$. Now, we require $b(p) \in \text{Im}\,\Phi^T(p))$. If it does

not, then project b onto $\mathrm{Im}\,\Phi^T(p))$ along $\mathrm{Ker}\,(\Phi(p))$ to obtain $\tilde{b}$. The new direction vector, e_{i+1}, is obtained as the natural projection of $\tilde{b}$ onto $\mathcal{M}$. In general e_{i+1} will not belong to $\mathcal{I}$. One implementation of these constructions is the following:

— Let $Q := \Phi^*\Phi$, where Φ^* is a right inverse of Φ. Then Q is a projection on $\mathrm{Im}\,\Phi^T(p)) = \mathrm{Im}\,(Q) = Q\mathcal{Y}$ along $\mathrm{Ker}\,\Phi(p)) = \mathrm{Ker}\,(Q) = (I-Q)\mathcal{Y}$. Thus $\tilde{b} = Qb$.

— Project this result onto $\mathcal{M}$ and renormalize to obtain $e_{i+1} = \alpha P\tilde{g}^t = \alpha PQg^t$ (α is the renormalization factor) which yields the recursion

$$e_{i+1} = \alpha PQP^t e_i. \tag{34}$$

Remarks:

1) Method 1 may converge if 1) there exists a μ^* which satisfies the necessary conditions for a closest static bifurcation point, 2) μ^* is a regular point of the bifurcation set Σ, and 3) Σ satisfies certain curvature conditions at μ^*, and 4) the search begins with a vector $\mu_0 = m_0 e_0$ sufficiently close to μ^*. This is essentially the method used in [68], [70] and detailed convergence conditions can be found in those references. In general, this method will not locate bifurcation points which are of higher codimension than one. Such points are not regular points of Σ. Recently, a method has been proposed that incorporates estimates of the curvature of σ to improve the convergence rate [71].
2) The conditions for convergence of method 2 are similar to those stated for method 1 except that the conditions 2) and 3) for regularity and curvature for the set Σ are replaced by conditions on the set $\mathcal{B}$. $\mathcal{B}$ is generally a smooth and regular submanifold of $\mathcal{Y}$ whereas Σ is typically badly structured as it can contain cusps and other nonregular structures. This method is useful for finding bifurcation points of higher codimension.

The following arguments provide some insight into the convergence properties of the algorithm.

Proposition 4: Let $p^* = (x^*, w^*, \mu^*) \in \mathcal{B}$ and let $U = \{p \in R^{2N+1} \mid \|p - p^*\|^2 < r^2\}$ be a spherical neighborhood of p^* in $\mathcal{Y}$. Suppose that $\|\mu^*\|^2 > 0$ is a unique extremum of $\|\mu\|^2$ contained in $\mathcal{B} \cap U$, and:

1) For each $p_0 = (x_0, w_0, \mu_0) \in U$, the Newton–Raphson–Seydel method converges to $p = (x, w, m\mu_0) \in \mathcal{B} \cap U$.
2) For each $p_1, p_2 \in \mathcal{B} \cap U$, the inequality

$$\|\alpha_1 PQ(e_1)P^t e_1 - \alpha_2 PQ(e_2)P^t e_2\| \le K\|e_1 - e_2\|,$$
$$\text{for some real number } K, 0 \le K < 1.$$

Then for any initial $p_0 \in U$, the algorithm converges to p^*.

Proof: Condition 2) states that (24) is a contraction. Thus conditions 1) and 2) together ensure that the recursion produces a well defined map $\mathrm{g} : \mathcal{B} \cap U \to \mathcal{B} \cap U$. To see this, consider a single iteration of the algorithm beginning with a point $\tilde{p} = (\tilde{x}, \tilde{v}, \tilde{m}, \tilde{e}) \in \mathcal{B} \cup U$. Now use (24) to update the search direction, so that $\tilde{e} \to \hat{e}$. The next step is application of the Newton–Raphson–Seydel method with starting value $\hat{p} = (\tilde{x}, \tilde{v}, \tilde{m}\hat{e})$. We need to show that $\hat{p} \in U$ so that 1) ensures convergence to $\mathcal{B} \cap U$. This requires direct calculation beginning with

$$\begin{aligned}\|\hat{p} - p^*\|^2 &= \|\tilde{x} - x^*\|^2 + \|\tilde{v} - v^*\|^2 + \|\tilde{m}\hat{e} - m^*e^*\|^2 \\ &= \|\tilde{p} - p^*\|^2 + \|\tilde{m}\hat{e} - m^*e^*\|^2 - \|\tilde{m}\tilde{e} - m^*e^*\|^2.\end{aligned}$$

Using the fact that $\hat{e}$, $\tilde{e}$, and e^* are unit vectors, it can be verified by direct computation that

$$\begin{aligned}&\|\tilde{m}\hat{e} - m^*e^*\|^2 - \|\tilde{m}\tilde{e} - m^*e^*\|^2 \\ &\quad = \tilde{m}m^*\{\|\hat{e} - e^*\|^2 - \|\tilde{e} - e^*\|^2\}\end{aligned}$$

with which we obtain

$$\|\hat{p} - p^*\|^2 = \|\tilde{p} - p^*\|^2 + \tilde{m}m^*\{\|\hat{e} - e^*\|^2 - \|\tilde{e} - e^*\|^2\}.$$

Since $\hat{e} = \tilde{\alpha}PQ(\tilde{e})P^T\tilde{e}$ and $e^* = \alpha^* PQ(e^*)P^T e^*$, condition 2) implies that $\|\hat{e} - e^*\| \le K\|\tilde{e} - e^*\|$. It follows that $\tilde{m}m^*\{\|\hat{e} - e^*\|^2 - \|\tilde{e} - e^*\|^2\} \le 0$, and hence we must have

$$\|\hat{p} - p^*\|^2 \le \|\tilde{p} - p^*\|^2 < r^2.$$

Consequently, $\hat{p} \in U$. Moreover, the fact that $\mathcal{B}$ is a smooth manifold and (10) is a contraction implies that g is a contraction. Any fixed point p' of g must satisfy $e' = PQP^t e'$. But then p' is an extremum of $\|m\|^2$, and by assumption p^* is the only extremal point contained in $\mathcal{B} \cap U$. □

Computing Unfoldings:

Lyapunov–Schmidt Reduction and Reduced Bifurcation Equation: Consider the map F: $R^n \times R^p \to R^n$, and for convenience assume that $(0,0) \in R^n \times R^p$ and it is a bifurcation point. Using the method of Lyapunov–Schmidt the study of the zeros of $F(x,\mu)$ can be reduced to the study of the zeros of the so-called (reduced) bifurcation equation, which typically involves only a few dependent variables. The essentials of the method of Lyapunov–Schmidt will be briefly reviewed in a somewhat simplified version that is adequate for our immediate needs. We give the more general construction below when addressing Hopf bifurcation [37], [41].

Define $J = D_x F(0,0)$ so that

$$F(x,\mu) = Jx + N(x,\mu) \tag{35}$$

where

$$N(0,0) = 0, \quad D_x N(0,0) = 0. \tag{36}$$

Thus we wish to study the solution set of the equation

$$Jx + N(x,\mu) = 0 \tag{37}$$

in a neighborhood of (0,0).

If J has rank r then there exist full rank matrices L, R of dimension $n \times r$ and $r \times n$, respectively, such that $J = LR$. Furthermore, L has a left inverse L^* and R has a right inverse R^*. Now, we can decompose $R^n = \mathrm{Ker}\,(R^{*T}) \otimes \mathrm{Im}\,(R^*)$. Let U be a matrix with $n-r$ columns that span $\mathrm{Ker}\,(R^{*T})$.[14] Thus we can define new coordinates $x \leftrightarrow (u, v)$ via the transformation

$$x = Uu + R^*v. \tag{38}$$

Proposition 5: Let W be a matrix with $n - r$ columns that span $\mathrm{Ker}\,(L^*)$, then (37) is equivalent to

$$\begin{aligned} v + L^*N(Uu + R^*v, \mu) &= 0 \\ W^TN(Uu + R^*v, \mu) &= 0 \end{aligned} \tag{39}$$

where $u \in R^{n-r}$, $v \in R^r$ are new coordinates as defined by (28).

Proof: This is a well known result that is easily obtained by substituting (38) into (37) and then premultiplying (37) by the nonsingular matrix

$$T = \begin{bmatrix} L^* \\ W^T \end{bmatrix}.$$

Note that nonsingularity follows from the fact that $R^n = \mathrm{Ker}\,(L^*) \oplus \mathrm{Im}\,(L^{*T})$. □

Applying the Implicit Function Theorem to the first equation in the proposition, we conclude that there is a (smooth) unique function $v^*(u, \mu)$ defined on a neighborhood of (0,0) which satisfies it. Thus on a neighborhood of (0,0) second equation of (39) becomes

$$f(u, \mu) := W^TN(Uu + R^*v^*(u, \mu), \mu) = 0. \tag{40}$$

Equation (40) is referred to as the *(reduced) bifurcation equation.*

Note also that the number of independent equations represented by (39) is $\tilde{r} := n - r$. It is easily verified that

$$f(0,0) = 0 \quad \text{and} \quad D_uf(0,0) = 0. \tag{41}$$

We will focus on the case $\tilde{r} = 1$ in which case (40) represents a single equation in one unknown.

5) The Unfolding: The zero structure of the family $F(x, \mu)$ near the singular point $(x, \mu) = (0, 0)$ is completely characterized by the zero structure of the reduced family $f(u, \mu)$ near the point $(u, \mu) = (0, 0)$.

Our goal is to investigate the zero structure of a given family $f(u, \mu)$ near its singular point (0,0). One obvious approach is to determine if the family $f(u, \mu)$ is equivalent to its universal unfolding at (0,0) (i.e., the universal unfolding of f_0). If so, we can infer all of the properties of $f(u, \mu)$ from an established catalog of unfoldings. To make this determination we seek an appropriate (near identity) transformation $(u, \mu) \to (z, \gamma)$, which reduces $f(u, \mu)$ to $\varphi(z, \gamma(\mu))$ such that on a neighborhood of (0,0), the zeros of φ coincide with those of f, the parameter γ is of some minimum dimension q, and φ is a polynomial of some degree in z. Thus the characterization of the zeros of the function $F(x, \mu)$ is ultimately reduced to the study of the much simpler problem

$$\varphi(z, \gamma) = 0, \quad \varphi\colon R^p \times R^q \to R^p. \tag{42}$$

In the case of $p = 1$, the following result is well known.

Proposition 6: Suppose that the reduced bifurcation (40) is smooth and that the first nonvanishing derivative is the rth with $r \geq 2$.

$$D_a^if(0,0) = 0, \quad i = 0, \ldots, r-1 \text{ and } D_a^rf(0,0) \neq 0. \tag{43}$$

Then 1) there exists a smooth change of variables $z = \mathbf{z}(a, \mu)$ and $\gamma_i = \gamma_i(\mu)$, $i = 0, \ldots, r-2$, so that (40) is reducible to the following polynomial equation on a neighborhood of $(a, \mu) = (0, 0)$

$$g_0(\mu) + g_1(\mu)z + \cdots + \gamma_{r-2}(\mu)z^{r-2} + z^r = 0 \tag{44}$$

2) if, in addition, $\frac{\partial\gamma(0)}{\partial\mu}$ is of full rank, then (40) is locally equivalent to the universal unfolding of $f_0(a)$

$$\varphi(z, \gamma) = \gamma_0 + \gamma_1 z + \cdots + \gamma_{r-2}z^{r-2} + z^r. \tag{45}$$

Proof: The Proposition is a variant of well known results [37, Section 6.8], [34, Section 4.1]. Conclusion 1) follows from the Malgrange Preparation Theorem and 2) from the Implicit Function Theorem. □

Remark: The condition that $\partial\gamma(0)/\partial\mu$ is of full rank is sometimes called a 'genericity condition.' If this condition obtains then the original family is 'richly parameterized' in the sense that variation of the original parameters can produce all possible zero patterns that can be generated by small perturbations of f_0. If $\partial_\gamma(0)/\partial\mu$ is degenerate, then even small changes in the model $F(x, \mu)$ are likely to alter the codimension of the singularity and change the way in which bifurcations associated with the singularity manifest themselves. We say the singularity is *generic* or *nongeneric*, respectively, if the genericity condition is satisfied or not satisfied.

In actual computation, the transformations are typically approximated using the Taylor expansion of $f(u, \mu)$ [37]. Let

$$\alpha_0(\mu) := f(0, \mu) = w_0^TF(0, \mu) \tag{46a}$$

and compute the derivatives

$$\begin{aligned} \alpha_1(\mu) &:= D_af(0, \mu) = \lim_{a \to 0} D_a[w_0^TF(0, \mu)] \\ &\vdots \\ \alpha_r(\mu) &:= D_a^rf(0, \mu) = \lim_{a \to 0} D_a^r[w_0^TF(0, \mu)] \end{aligned} \tag{46b}$$

[14] If we take $R^* = R^T(RR^T)^{-1}$, then $\mathrm{Ker}\,(R^{*T}) \sim \mathrm{Ker}\,(R)$. Similarly, if $L^* = (L^TL)^{-1}L^T$, then $\mathrm{Ker}\,(L^*) \sim \mathrm{Ker}\,(L^T)$.

and stop at that value of r for which

$$\alpha_0 = 0, \ldots, \alpha_{r-1} = 0, \alpha_r \neq 0. \tag{47}$$

The following approximation Proposition provides the required construction.

Proposition 7: Suppose that $f(u, \mu)$ is smooth and that (47) holds. Then $f(u, \mu) = 0$ is equivalent to $g(z, \mu)$, on a neighborhood of $(a, \mu) = (0, 0)$, where

$$g(z, \mu) = \gamma_0(\mu) + \gamma_1(\mu)z + \cdots + \gamma_{r-2}(\mu)z^{r-2} + z^r + o(|z|^r) \tag{48}$$

and

$$z = a - \frac{\alpha_{r-1}(\mu)}{\alpha_r(\mu)} + o(|\mu|), \quad \gamma_s(\mu) = r!\frac{\delta_s(\mu)}{\alpha_r(\mu)} \quad \text{for } s = 0, \ldots, r-2 \tag{49a}$$

$$\delta_s(\mu) = \sum_{j=s}^{r} \frac{\alpha_j(\mu)}{j!}\binom{j}{s}\left(\frac{-\alpha_{r-1}(\mu)}{\alpha_r(\mu)}\right)^{j-s} + o(|\mu|^{r-s}). \tag{49b}$$

Proof: Direct computation. □

Remark: Notice that the unfolding given above describes a bifurcation of codimension $r-1$ the bifurcation surfaces in the unfolding parameter $(\gamma-)$ space are simply $\gamma_i = 0$, $i = 0, \ldots, r-2$. In the physical parameter $(\mu-)$ space the surfaces are defined by $\gamma_i(\mu) = 0$. Each of these $r-1$ functions defines a codimension one surface. These surfaces intersect to define higher codimension manifolds, the highest codimension being $r-1$ which is the intersection of all of them. The normal vector to the surface at any μ on it is defined by $\gamma_i(\mu)$ is $D_\mu\gamma_i(\mu)$. If $r = 2$, so that the bifurcation is a saddle-node, then it is easy to show that $D_\mu\gamma_0(\mu) = D_\mu\alpha_0(\mu) = w^T F_\mu(0, \mu)$. The significance and utility of this observation is developed in [16], [57].

6) Static Bifurcation and Voltage Stability: By the early 1980's various factors had caused power system operators to seek maximum utilization of the transmission network. Previously unobserved stability related difficulties emerged and a vigorous effort was made to understand them and find remedies [73]. Typically, these problems involved the inability to maintain load bus voltage magnitudes and became referred to as voltage instabilities. Static bifurcation of the load flow equations is an appealing formalization of voltage stability because it embodies key characteristics associated with real voltage instability events: the presence of multiple equilibria, a relationship between dynamic stability and voltage collapse, a high degree of sensitivity of certain bus variables to control parameters, and a relatively long period of drift prior to collapse. Of course, static bifurcation intrinsically involves multiple equilibria so we will confine our brief remarks to the latter three points.

7) Static Bifurcation and Dynamic Stability: Bifurcating equilibria can be (asymptotically) stable in the sense of Lyapunov. We have seen examples of this. This type of stability is not meaningful in a practical sense because even an arbitrarily small perturbation of the dynamics can render it unstable in the sense of Lyapunov or can anihilate the equilibrium point altogether. A practical concept of stability of an equilibrium point requires that the flow is locally structurally stable at the equilibrium point and that the equilibrium point is stable in the sense of Lyapunov. We use the term *practical stability*[15] for equilibria that satisfy these conditions. Recall that Proposition 1 states that local structural stability implies that the equilibrium point is causal and hyperbolic. Thus practical stability of an equilibria point implies that it is causal and hyperbolic. But for causal, hyperbolic equilibria Lyapunov stability can be ascertained from the ordinary differential (7) which has linearization

$$\delta\dot{x} = A\delta x, \text{ with } A := [D_x f - D_y f(D_y g)^{-1} D_x g]^* \tag{50}$$

where * denotes evaluation at the equilibrium point. The equilibrium point is stable in the sense of Lyapunov only if all of the eigenvalues of A have nonpositive real parts, and hyperbolicity further restricts the eigenvalues to the open left hand plane. Thus practical stability implies exponential stability.

We can easily show that static bifurcation points are not stable in the sense of practical stability. Practical stability implies causality which allows us to apply Schur's formula to write the determinant of the load flow equations

$$\det\{J\}^* = \det\{A\}\det\{D_y g\}^*. \tag{51}$$

From this, we see that a (causal) static bifurcation point corresponds to $\det\{A\}^* = 0 = \det\{-A\}^*$. Hence, static bifurcation points are not stable in the sense of practical stability, since the latter requires $\det\{-A\}^* > 0$.

Venikov *et al.* [6] recognized the significance of a degeneracy in J with respect to the steady state stability of a power system. They observed that under certain conditions a change the sign of $\det\{J\}$ during a continuous variation of system states and parameters coincides with the movement of a real characteristic root of the linearized swing equations across the imaginary axis into the right half of the complex plane. Thus they recommended tracking $\det\{J\}$ during load flow calculations and proposed a modification of Newton's method which allows precise determination of the parameter value where such a sign change occurs. Tamura *et al.* [75] discuss some computational experience using this method.

8) Bus Variable Sensitivities: A discussion of the significance of a degeneracy in J in terms of bus variable sensitivities was given by Abe *et al.* [76]. We see from the Lyapunov–Schmidt analysis, that in the (u, v) coordinates, the sensitivities of the v variables are well behaved. Simply differentiate the first equation of (39) to obtain (at (0,0))

$$D_\mu v(0, 0) = -L^* D_\mu N(0, 0). \tag{52}$$

[15] Practical stability as used here is related to but not identical with the notion of practical stability in [74].

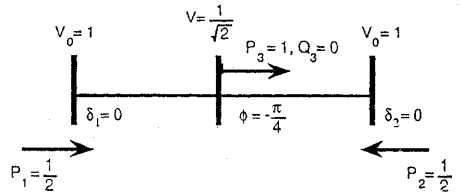

Fig. 7. Equilibrium conditions illustrating impending voltage collapse.

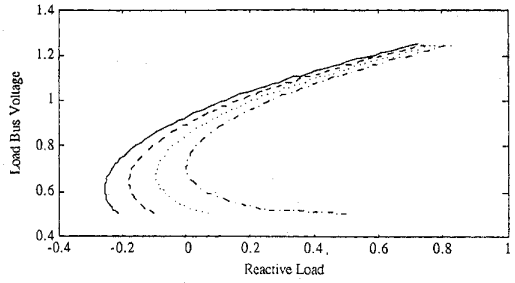

Fig. 8. Voltage-power characteristics illustrate how the load bus voltage V varies as a function of reactive load Q_3 for several values of real power load P_3. From left to right $P_3 = .7, .8, .9, 1.0$. These curves are obtained with $\Delta P = 0, B = 0$.

However, derivatives $D_\mu u$ are indeterminant. These are the sensitive variables. It follows that the sensitive physical variables can be identified from the basis vectors for $\mathrm{Ker}(J)$. Specifically, components of x that correspond to nonvanishing elements in the basis vectors are highly sensitive to parameter variations—indeed their sensitivities to parameter change tend to infinity as the parameter value approaches its bifurcation value. The magnitudes of the elements in the basis vectors is useful for identifying the relative participation of the system dependent variables.

9) Slow Time Scale Behavior: Dobson and Chiang [15] discuss the dynamical behavior associated with a saddle node bifurcation. At a generic saddle-node bifurcation point the equilibrium point has a 1-D center manifold (see Fig. 4). Motion on the center manifold is such that trajectories beginning on it from one side of the equilibrium point approach the equilibrium point, and trajectories on the other side diverge from it. The convergent trajectory, of course takes infinite time to reach the equilibrium, and the rate of divergence of the divergent trajectory approaches zero near the equilibrium. Trajectories beginning off the center manifold but near it exhibit similar behavior—a slow approach followed by a slow divergence. Post bifurcation behavior is similar as well. Even though there is no longer an equilibrium point, its "fingerprint" is clearly evident.

Example 1 Revisited: Let us now return to the system of Example 1. Consider the parameter values

$$\mu = [\Delta P, B, P_3, Q_3]^t = [0, 0, -1, 0]^t \tag{53}$$

which results with an equilibrium point at $(\theta^*, \phi^*, V^*) = (0, -\pi/4, 1/\sqrt{2})$. The line diagram in Fig. 7 illustrates the equilibrium power flow.

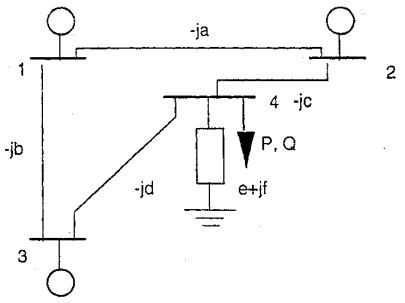

Fig. 9. A four bus system with load characterized as a mixed constant admittance and constant power load.

Further analysis based on the calculations described above reveal that the bifurcation is of codimension 1 with universal unfolding as given by (45). We also compute the null space spanning vector $u_0 = [0, \sqrt{2}, -1]^t$ and the approximate transformation relation

$$\gamma_0(\mu) = -\frac{\Delta P}{4} - \frac{B}{4}\left(1 + \frac{B}{4}\right) + \frac{P_3 - 1}{2} + \frac{Q_3}{2}. \tag{54}$$

It follows from the structure of u_0 that we may anticipate observation of the bifurcation in the variables ϕ or V but not in θ. Also in view of the relation between the physical parameters, μ, and the bifurcation parameter γ_0 we may trigger the collapse by decreasing ΔP and B or by increasing P_3 and Q_3. These facts justify analysis of this voltage collapse scenario in terms of load bus voltage-power (either real or reactive) curves, a classical procedure widely used in contemporary power system operations. For the present example, these curves are illustrated in Fig. 8.

Example 5: (Higher Order Singularities and Load Models): In order to further illustrate the concepts and the computations discussed above, consider the example system [77] that consists of three machines and four buses with combined constant admittance and P-Q load shown in Fig. 9.

10) Constant Admittance Load: With the constant admittance load, the load bus can be treated as an internal bus and eliminated in the usual way by defining a reduced network admittance matrix. We assume uniform damping. The translational symmetry in the three resulting second order differential equations allows reduction to two equations by specifying bus one as a swing bus and defining the relative angles

$$\theta_1 := \delta_2 - \delta_1, \quad \theta_2 := \delta_3 - \delta_1. \tag{55}$$

Thus we obtain

$$\ddot{\theta}_1 + \gamma\dot{\theta}_1 + 2B_{12}\sin(\theta_1) + B_{23}\sin(\theta_1 - \theta_2) + B_{13}\sin(\theta_2) + C_{23}\cos(\theta_2 - \theta_1) - C_{13}\cos(\theta_2) = \Delta P_1 \tag{56a}$$

$$\ddot{\theta}_2 + \gamma\dot{\theta}_2 + 2B_{13}\sin(\theta_2) + B_{23}\sin(\theta_2 - \theta_1) + B_{12}\sin(\theta_1) + C_{23}\cos(\theta_2 - \theta_1) - C_{12}\cos(\theta_1) = \Delta P_2 \tag{56b}$$

where $\Delta P_1 = P_2 - P_1$ and $\Delta P_2 = P_3 - P_1$.

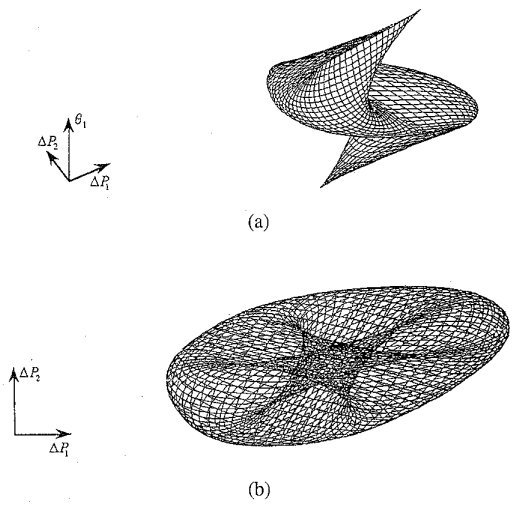

Fig. 10. (a) A view of the equilibrium surface of (56) with $B_{12} = B_{13} = B_{23} = 1$, $C_{12} = C_{13} = C_{23} = .15$. The vertical axis corresponds to the variable θ_1 and the horizontal plane is the parameter plane $\Delta P_1 - \Delta P_2$. The surface consists of the component corresponding to $-\pi \leq \theta_1 \leq \pi$. The edge along the top is parallel to the horizontal plane. There is a symmetrical edge along the bottom so that the surfaces stack up and down the vertical axis, connecting along these edges, to provide the 2π periodicity in θ_1 that is expected. (b) By looking straight down at the surface onto the parameter plane without hidden line removal, the well known star pattern that divides the parameter space is revealed. Outside the egg shaped region, there are no equilibria, crossing into the egg there are 2, within the star points there are 4, and in the center region there are 6. These conclusions are readily confirmed by careful examination of the equilibrium surface in Fig. 2(a). The boundary of the egg and the edges of the star are clearly bifurcation points.

Tavora and Smith [15] analyze the equilibrium solution structure of these equations (without transfer conductances) as a function of the two parameters ΔP_1 and ΔP_2.[16] It is useful to review some of their conclusions. Tavora and Smith show that the parameter space (the $\Delta P_1 - \Delta P_2$ plane) partitions into regions and within each region the number of equilibrium solutions is 0, 2, 4, or 6. Fig. 10(a) and (b) illustrate this, but in the present example, the calculations were performed for a system with transfer conductances. Fig. 10(a) shows the equilibrium surface associated with (56). By looking straight down at the surface, as in Fig. 10(b), without removing hidden lines, the regions identified by Tavora and Smith are clearly visible.

If we ignore all transfer conductances ($C_{ij} = 0$) and set $B_{ij} = 1$, then this system reduces to one whose global equilibium properties where analyzed in detail by Tavora and Smith. The equilibrium equations are

$$2\sin(\theta_1) + \sin(\theta_1 - \theta_2) + \sin(\theta_2) - \Delta P_1 = 0 \tag{57a}$$

$$2\sin(\theta_2) + \sin(\theta_2 - \theta_1) + \sin(\theta_1) - \Delta P_2 = 0. \tag{57b}$$

[16] Another approach to the study of equilibrium point structure of lossless power systems is given in [78].

There are several bifurcation points which appear as cusps in the $\Delta P_1 - \Delta P_2$ plane. One of these corresponds to $\theta_1 = \pi/2, \theta_2 = \pi, \Delta P_1 = 1, \Delta P_2 = 2$. The algorithm locates this point from appropriate initial conditions. Further computer analysis to classify this bifurcation point establishes that the dimension of the kernel of the Jacobian is one, but fails to identify an integer $k \in \{1, \ldots, k_{\max}\}$ for which $\alpha_k > \epsilon$. Note that $k_{\max}$ and ϵ are parameters which must be set consistent with available computational precision. The point is that within our computational precision it was not possible to identify an $\alpha_k \neq 0$. Hand calculations confirm that this is a codimension ∞ bifurcation point. This indicates the high degree of symmetry and degeneracy associated with this idealized system.

Now we consider a case with transfer conductances, retaining $B_{ij} = 1$, we set $C_{ij} = 0.15$. A bifurcation point is found with $\theta_1 = 1.64962$, $\theta_2 = 3.13274$, $\Delta P_1 = 1.16961$, $\Delta P_2 = 2.03570$. The sequence of coefficients $\alpha_0 = 0.000$, $\alpha_1 = 0.000$, $\alpha_2 = 0.000$, $\alpha_3 = 0.026$ indicates a singularity of codimension 2. We further obtain the parameter sensitivity matrix

$$\frac{\partial \gamma(\mu^*)}{\partial \mu} = \begin{bmatrix} 167.22 & -100.22 \\ 0 & 0 \end{bmatrix}$$
$$\mu = [\Delta P_1, \Delta P_2]. \tag{58}$$

Notice that although the singularity is of codimension 2 and hence it is generic in two parameter families, the particular two parameter family defined by (57) does not represent a versal unfolding of the singularity. This means that not all changes in the equilibrium point structure that might be induced by small perturbations of the equations will be observed by varying the parameters $\Delta P_1, \Delta P_2$.

11) Mixed Load: We consider a combination of constant admittance and constant impedance loads. In this case, the load bus must be retained, but the translational symmetry allows specification of a swing bus. The resultant set of differential-algebraic equations are of the form

$$\begin{aligned} &\ddot{\theta}_1 + 2B_{21}\sin(\theta_1) - B_{24}V_4\sin(\theta_3 - \theta_1) \\ &\qquad + B_{13}\sin(\theta_2) = \Delta P_1 \\ &\ddot{\theta}_2 + 2B_{31}\sin(\theta_2) - B_{34}V_4\sin(\theta_3 - \theta_2) \\ &\qquad + B_{12}\sin(\theta_1) = \Delta P_2 \\ &B_{42}V_4\sin(\theta_3 - \theta_1) + B_{43}V_4\sin(\theta_3 - \theta_2) - P_4 = 0 \\ &B_{42}V_4\cos(\theta_3 - \theta_1) + B_{43}V_4\cos(\theta_3 - \theta_2) \\ &\qquad - B_{44}V_4^2 + Q_4 = 0 \end{aligned} \tag{59}$$

where $\Delta P_1 = P_2 - P_1$ and $\Delta P_2 = P_3 - P_1$. We consider the case in which $B_{12} = B_{13} = 1$, $B_{24} = B_{34} = 2$, $B_{44} = -4$, and $B_{ij} = B_{ji}$.

Computation identifies a singular point at $\theta_1 = 1.5709005$ $(\approx \pi/2), \theta_2 = 3.1415926$ $(\approx \pi), \theta_3 = 2.3562465$, $V_4 = .70714361$, $\Delta P_1 = 1$, $\Delta P_2 = 2$, $P_4 = 0, Q_4 = 0$. The null space spanning vector is

determined to be

$$u = \begin{bmatrix} 0.8528 \\ 0.0000 \\ 0.4264 \\ 0.3015 \end{bmatrix}$$

and the sequence of coefficients $\alpha_0 = 0.000$, $\alpha_1 = 0.000$, $\alpha_2 = 0.000$, $\alpha_3 = 0.372$; indicating a singularity of codimension 2. We further obtain the parameter sensitivity matrix

$$\frac{\partial \gamma(\mu^*)}{\partial \mu} = \begin{bmatrix} -8.596 & 4.298 & -2.149 & -6.446 \\ 0 & 0 & 0 & 0 \end{bmatrix}$$
$$\mu = [\Delta P_1, \Delta P_2, P_4, Q_4]. \tag{60}$$

Once again, we see that that the local family defined by (59) is not versal. It is easy to verify that this will always be the case when the parameters enter the equations linearly.

12) Voltage Dependent Load: It has long been recognized that the constant admittance and constant power load models represent only crude approximations to actual load behavior and that more precise load models may be necessary for accurate characterization of voltage stability issues. Proposed refinements include static representation of frequency and voltage dependence and, in some cases, the inclusion of load dynamics. Such modifications are readily accommodated within the bifurcation framework. In the present instance, we wish to show that even a simple expansion of the load model can have a significant qualitative effect.

We replace the constant reactive load of the previous example with the voltage dependent model

$$Q_4(V_4) = Q_{40}V_4, Q_{40} \quad \text{a constant.} \tag{61}$$

By so doing, it is determined that the singular point identified above remains a singular point, the null space spanning vector and the codimension are unchanged. However, the parameter sensitivity matrix is

$$\frac{\partial \gamma(\mu^*)}{\partial \mu} = \begin{bmatrix} -8.596 & 4.298 & -2.149 & -11.005 \\ 0 & 0 & 0 & -1.944 \end{bmatrix}$$
$$\mu = [\Delta P_1, \Delta P_2, P_4, Q_{40}]. \tag{62}$$

The significance of this result is that the system with the voltage dependent load represents a versal unfolding of the singularity.

Example 6: (Real Power Transfer Limits): The increased importance of megawatt transfer between areas has spawned the development of methods for the identification of the limits of feasible transfers as dictated by the voltage and thermal constraints under both normal and contingency outage operation. Although there are numerous methods for identifying regions of secure power transfers under transmission line loading and voltage magnitude constraints, work on the identification of feasible megawatt transfers (i.e., the set of all megawatt transfers which guarantee the existence of a voltage profile) has only been considered recently [79]–[81]. This is an excellent example of how static bifurcation analysis can be used to address important applications issues by appropriate definition of the parameter space. We will outline the key ideas.

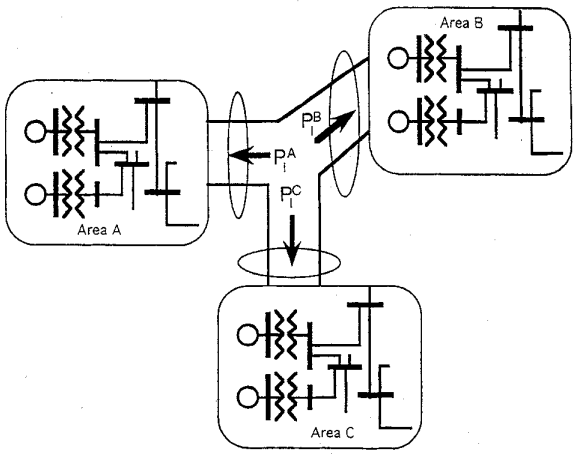

Fig. 11. The three-area power system.

As in the above references, we consider a classical power system model (2), in which the equilibrium equations can be explicitly written

$$f_i = \sum_{j=1}^{N_s} [V_i V_j B_{ij} \sin(\delta_i - \delta_j) + V_i V_j G_{ij} \times \cos(\delta_i - \delta_j)] - P_i,$$
$$i \in I_{\text{Total}} = \{1, \ldots, N_B = n_g + n_{PV} + n_{PQ}\} \tag{63a}$$
$$g_i = \sum_{j=1}^{N_B} [V_i V_j G_{ij} \sin(\delta_i - \delta_j) - V_i V_j B_{ij} \times \cos(\delta_i - \delta_j)] - Q_i, \quad i \in I_{PQ}. \tag{63b}$$

These comprise $N = n_g + n_{PV} + 2n_{PQ}$ equations. The N unknowns are the $n_g + n_{PV} + n_{PQ}$ bus angles and the n_{PQ} PQ-bus voltage magnitudes. As parameters, we could consider any subset or combinations of the injections P_i, Q_i, transmission line parameters B_{ij}, G_{ij} and voltage magnitudes V_i corresponding to generator and PV buses. The transfer limit problem suggests a particular choice of parameter space.

The interarea megawatt transfer problem considered here is based on the interconnected three-area power system model shown in Fig. 11 where P_I^A, P_I^B, P_I^C denote the net megawatt (MW) imports into areas A, B and C, respectively. Since $P_I^A + P_I^B + P_I^C = 0$, only two of these are independent so the real power interchange space (i.e., the $\mathbf{P_I}$-space) may be considered the $P_I^A - P_I^B$ plane shown in Fig. 12. We wish to regulate the real power flow between areas (of course, we can only regulate two of the three). This is accomplished indirectly by adjusting the real power

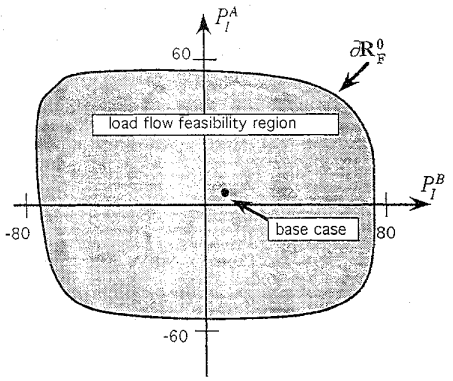

Fig. 12. Example of a load-flow feasibility region in the interarea MW imports space.

injections at generator buses.[17] We assume that the swing bus is located in Area C and there is at least one generator in each area A and B. To explicitly show the effect of generator injections on real power imports we can compute

$$P_I^A = \sum_{\substack{j \in I_B \cup I_C \\ i \in I_A}} \left[\frac{1}{2}(V_i^2 - V_j^2)G_{ij} - V_i V_j B_{ij} \sin(\delta_i - \delta_j) \right] \tag{64a}$$

$$P_I^B = \sum_{\substack{j \in I_A \cup I_C \\ i \in I_B}} \left[\frac{1}{2}(V_i^2 - V_j^2)G_{ij} - V_i V_j B_{ij} \sin(\delta_i - \delta_j) \right] \tag{64b}$$

where I_A, I_B, I_C are the bus index sets for areas A, B, C. Now, we can replace two of the equations in the set (63a) by (64a) and (b). In fact, it is easy to see, that independence of the controllable parameters is maintained if they replace one generator equation in area A, and one generator equation in area B.

We assume that all load parameters, transmission line parameters, independent voltage parameters and all generator real power injections[18] other than the two replaced generators (and the swing bus) are fixed. Then the modified set of load flow equations take the form

$$F(x, P_I^A, P_I^B) = F_0(x) + u(P_I^A, P_I^B) = 0. \tag{65}$$

Now, we are in a position to study the load flow solution structure as a function of the MW interchange parameters.

In this discussion, we neglect all operating constraints dictated by the thermal, voltage magnitude, and reactive injection limits, so the problem of identifying the domain of feasible interarea MW transfer reduces to the problem of identifying the (static) bifurcation set of the load-flow equations (53) in the $\mathbf{P_I}$-space. Recall that under the usual conditions, (55) defines a regular manifold $\mathcal{E}$ of equilibrium points in $R^N \times \mathbf{P_I} = R^{N+2}$. The bifurcation points form codimension 1 submanifolds (possibly intersecting) that divide $\mathcal{E}$ into open regions called *sheets*. Let $(x^0, \mathbf{P}_I^0) \in \mathcal{E}$ denote a base case operating point and suppose it belongs to the sheet $\mathcal{E}^0$.

Definition 6: The load flow feasibility region at $(x^0, \mathbf{P}_I^0)$, denoted $\mathbf{R}_F^0$, is the natural projection of $\mathcal{E}^0$ onto $\mathbf{P_I}$.

Points on the boundary of $\mathbf{R}_F^0$, denoted $\partial \mathbf{R}_F^0$, belong to the bifurcation set. The notion of a load flow feasibility region in this spirit goes back to [3], [66]. The key to obtaining the graphical representation of $\mathbf{R}_F^0$ is finding the boundary of $\partial \mathbf{R}_F^0$. One approach to finding this $\partial \mathbf{R}_F^0$ is described in [80], [81]:

1) Obtain a feasible base-case point,
2) radial search at specified angles to obtain boundary points, and
3) connect the boundary points using straight line segments.

Step 2) can be accomplished with a one-parameter static bifurcation calculation as described in Section III-A. A typical result illustrated in Fig. 12. A detailed application to the Klos–Kerner 11 bus test system is described in [80].

B. Hopf and Generalized Hopf Bifurcation

Oscillations associated with instability in the power systems are well known and frequently described in an extensive literature which spans several decades. However, the connection with bifurcation analysis has been developed only recently. Van Ness *et al.* [82] suggest that an observed oscillation is associated with a Hopf bifurcation. Abed and Varaiya [83] illustrate subcritical Hopf bifurcations in several electric power system models. Alexander [84] provides a thorough local stability analysis of Hopf bifurcations for a model of two machines connected with a lossy transmission line and demonstrates the occurrence of both subcritical and supercritical Hopf bifurcations. An example of Hopf bifurcation in a three machine classical network with lossy lines is given by Kwatny *et al.* [77], [85]. Another example is given by Rajagopalan *et al.* [86] in which a three machine system is modeled with a two-axis representation and excitation is included. Iravani and Semlyen [87] show Hopf bifurcation in a single machine system with a flexible turbine-generator shaft. Chen and Varaiya [88] illustrate a degenerate Hopf bifurcation in a two generator network with excitation and an infinite bus. Venkatasubramanian *et al.* [25] illustrate a different type of degenerate Hopf (double zero eigenvalues) in a single line network including a generator with voltage control (either excitation or a thyristor controlled reactance) and a constant power load. Subcritical and supercritical Hopf bifurcations are naturally encountered in studies of chaos in power systems [2], [89]. One could justifiably conclude that Hopf bifurcations are pervasive in power systems.

As we will describe, Hopf bifurcations in power systems can be analyzed using the same basic tools as static

[17] For our purposes here a generator bus is essentially a PV bus with controllable P.

[18] This is, of course, not necessary. An equivalent condition is to assume a set of generator participation factors is available from a dispatch program. See the references.

bifurcations, namely, the Newton–Raphson–Seydel method and the Lyapunov–Schmidt reduction.

1) Locating Hopf Bifurcation Points: Variants of the Newton–Raphson–Seydel method can be used to locate Hopf bifurcation points [90]. We will apply this method to the DAE (1). Thus we need to locate an equilibrium point

$$F(x,\mu)=0 \tag{66}$$

which is causal and so that the linearization of (7) has a pair of purely imaginary conjugate roots

$$\det\{j\omega\mathcal{I}_{n,m}-J(x,\mu)\}=0$$

where

$$\mathcal{I}_{n,m}=\begin{bmatrix} I_n & 0_{n\times m}\\ 0_{m\times n} & 0_m\end{bmatrix}. \tag{67}$$

As in the static case, we prefer to reformulate (67) as

$$w^T[J(x,\mu)-j\omega\mathcal{I}_{n,m}]=0$$

or

$$[J(x,\mu)-j\omega\mathcal{I}_{n,m}]v=0 \tag{68}$$

along with the requirement that w or v is nontrivial. Since $w\,(v)$ is complex, we can write it in polar form, $w_i=\delta_i e^{j\phi_i}(v_i=\delta_i e^{j\phi_i})$, and require

$$\sum_{i=1}^{n+m}\delta_i^2=1 \quad\text{and}\quad \sum_{i=1}^{n+m}\phi_i=0. \tag{69}$$

Equivalently, we can state the nontriviality requirement

$$w^T F_\mu(x,\mu)=1 \quad\text{or}\quad F_\mu(x,\mu)v=1. \tag{70}$$

2) Computing Unfoldings: As in the case of static bifurcations, we want to determine the important qualitative characteristics associated with Hopf bifurcation, e.g., the number and stability characteristics of period trajectories, as well as to characterize the bifurcation surfaces in the physical parameter space. There are two basic approaches: compute the center manifold and normal form and study the unfolding of the normal form (see Table 2), or use a variant of the Lyapunov–Schmidt reduction in which a reduced bifurcation equation needs to be computed, and from which the desired information can also be obtained. Hopf bifurcations are studied from the former point of view in [21], [34] and from the latter in [37], [41]. In terms of power system applications, there is simply not enough experience to prefer one approach over the other.

3) Lyapunov–Schmidt Reduction—A Second Look: In dealing with Hopf bifurcations we need a more general formulation of the Lyapunov–Schmidt reduction that applies to mappings on infinite dimensional spaces. Consider Φ to be a map between (possibly infinite dimensional) complete linear vector spaces $\mathcal{H}$ and $\mathcal{Y}$; $\Phi:\mathcal{H}\times R^p\to\mathcal{Y}$. We seek to characterize the solution set of $\Phi(x,\mu)=0$ near $(0,0)\in\mathcal{H}\times R^p$, which we write as

$$\Phi(x,\mu)=Lx+N(x,\mu)=0 \text{ with } L:=D_x\phi(0,0). \tag{71}$$

Let P: $\mathcal{H}\to\mathcal{H}$ and Q: $\mathcal{Y}\to\mathcal{Y}$ denote projection operators[19] with $\mathrm{Im}(P)=\mathrm{Ker}(L)$ and $\mathrm{Im}(Q)=\mathrm{Im}(L)$. Then we can split $\mathcal{H}$ and $\mathcal{Y}$,

$$\mathcal{H}=\mathrm{Im}(P)\oplus\mathrm{Im}(I-P) \tag{72}$$

$$\mathcal{Y}=\mathrm{Im}(Q)\oplus\mathrm{Im}(I-Q). \tag{73}$$

We can state the following well known theorem:

Proposition 8: Let P: $\mathcal{H}\to\mathcal{H}$ and Q: $\mathcal{Y}-\mathcal{Y}$ denote projection operators with $\mathrm{Im}(P)=\mathrm{Ker}(L)$ and $\mathrm{Im}(Q)=\mathrm{Im}(L)$. Then

1) (72) is equivalent to

$$Lv+QN(u+v,\mu)=0 \tag{74a}$$

$$(I-Q)N(u+v,\mu)=0 \tag{74b}$$

with

$$x=u+v, v=Px\in\mathrm{Im}(P), v=(I-P)x\in\mathrm{Im}(I-P)$$

2) there exists a linear map K: $\mathrm{Im}(Q)\to\mathrm{Im}(I-P)$, called the right inverse of L, such that $LK=I$ on $\mathrm{Im}(Q)$ and $KL=I-P$ on $\mathcal{H}$ so that (9a) is equivalent to

$$v+KQN(u+v,\mu)=0. \tag{75}$$

Proof: See [37], [41]. □

Once again, the Implicit Function Theorem applied to (75) assures the existence of a unique function $v^*(u,\mu)$ defined on a neighborhood of $(0,0)\in\mathcal{H}\times R^p$ that satisfies it. Moreover, $v^*(0,0)=0$. Substituting this function in (74b) yields the reduced bifurcation equation

$$(I-Q)N(u+v^*(u,\mu),\mu)=0. \tag{76}$$

In our applications, the subspaces $\mathrm{Im}(P)$ of $\mathcal{H}$ and $\mathrm{Im}(I-Q)$ of $\mathcal{Y}$ will be of finite dimension $\tilde{r}$, in which case (74) reduces to $\tilde{r}$ scalar equations in $\tilde{r}$ unknowns.

4) The Reduced Bifurcation Equation: Following [41], we will apply the Lyapunov–Schmidt method to analyze a Hopf bifurcation which has been located as above. For convenience, we assume that the bifurcation occurs at the point $(x,\mu)=(0,0)$ and that $\omega=1$. Now, we rescale time via the transformation $s=(1+\tau)t$ where τ is a

[19] Recall that if $\mathcal{H}=\mathcal{R}\otimes\mathcal{S}$, then there is a map Q: $\mathcal{H}\to\mathcal{H}$, called the projection on $\mathcal{R}$ along $\mathcal{S}$, such that for each $x=r+s$, $Qx=r$. Clearly, $\mathrm{Im}(Q)=\mathcal{R}$ and $\mathrm{Ker}(Q)=\mathcal{S}$. A map Q: $\mathcal{H}\to\mathcal{H}$ is a projection on $\mathrm{Im}(Q)$ along $\mathrm{Ker}(Q)$ if $Q^2=Q$.

new parameters introduced to keep the frequency of the oscillation (in the new time scale) at unity as parameters vary. Then, in terms of s we can write the system equations in the form

$$\Phi(x,\mu,\tau) := -(1+\tau)\mathcal{I}_{n,m}\frac{dx}{ds} + Jx + N(x,\mu) = 0. \quad (77)$$

We seek 2π-periodic solutions of (77). Hence, we consider $\mathcal{H}$ and $\mathcal{Y}$ to be spaces of suitably smooth 2π-periodic functions of s, and Φ is a map from $\mathcal{H} \times R^p \times R$ to $\mathcal{Y}$. Its linear part L: $\mathcal{H} \to \mathcal{Y}$ is

$$L := \Phi_x(0,0,0) = -\mathcal{I}_{n,m}\frac{d}{ds} + J. \quad (78)$$

To compute the reduced bifurcation equation, we need to determine a basis for each of the 2-D subspaces $\mathrm{Im}(P)$ of $\mathcal{H}$ and $\mathrm{Im}(I-Q)$ of $\mathcal{Y}$. For $\mathrm{Im}(P) = \mathrm{Ker}(L)$, we note that $Lx = 0$ has two 2π-periodic solutions

$$w_1(s) = \mathrm{Re}(e^{is}w), \quad w_2(s) = \mathrm{Im}(e^{is}w)$$

where

$$[-i\mathcal{I}_{n,m} + J]w = 0. \quad (79)$$

Similarly, we can take $\mathrm{Im}(I-Q) = \mathrm{Ker}(L^*)$ where the adjoint map is

$$L^* := \mathcal{I}_{n,m}\frac{d}{ds} + J^T. \quad (80)$$

Let W^* denote the eigenvector of L^* associated with eigenvalue i so that the two basis functions for $\mathrm{Im}(I-Q)$ are

$$w_i^*(s) = \mathrm{Re}(e^{is}w^*), \quad w_2^*(s) = \mathrm{Im}(e^{is}w^*). \quad (81)$$

Now, we write $u = w_1(s)u_1 + w_2(s)u_2$, and define[20]

$$\phi_i(u_1,u_2,\mu,\tau) := \langle w_i^*(s), \tilde{N}(w_1(s)u_1 + w_2(s)u_2, v^*(u_1,u_2,\mu,\tau)\mu,\tau\rangle \quad i = 1,2 \quad (82)$$

where

$$\tilde{N}(u,v,\mu,\tau) = -\tau\mathcal{I}_{n,m}\frac{d}{ds}(u+v) + N(u+v,\mu). \quad (83)$$

The following proposition establishes the form of (82).

Proposition 9: The reduced bifurcation equation has the form

$$\phi(u_1,u_2,\mu,\tau) = p(u_1^2+u_2^2,\mu,\tau)\begin{bmatrix}u_1\\u_2\end{bmatrix} + q(u_1^2+u_2^2,\mu,\tau)\begin{bmatrix}-u_2\\u_1\end{bmatrix} \quad (84)$$

[20]The inner product used for 2π-periodic functions is $\langle v_1, v_2\rangle = \frac{1}{2\pi}\int_0^{2\pi}\bar{v}_1^T(s)v_2(s)ds$ where the overbar denotes complex conjugate.

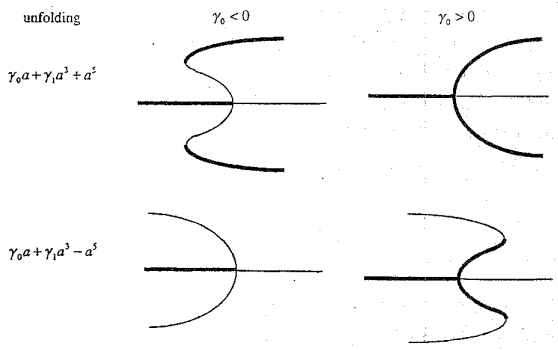

Fig. 13. Bifurcation diagrams for the codimension 2 Hopf bifurcation in terms of parameter γ_1. Each diagram plots the oscillation amplitude a versus γ_1. Bold denotes stable. Note that in some regions there are two periodic trajectories, one stable and one unstable.

with the scalar functions p and q satisfying

$$p(0,0,0) = 0 \quad \text{and} \quad p_\tau(0,0,\tau) = 0 \quad (85a)$$
$$q(0,0,0) = 0 \quad \text{and} \quad q_\tau(0,0,\tau) = -1. \quad (85b)$$

Proof: [41], see Proposition 2.3 in Chap. 8. □

It follows from (84) that nontrivial solutions of the reduced bifurcation equation ($\phi = 0$) exist only if $p = q = 0$. The form of p and q suggest a transformation to polar coordinates: $u_1 = a\cos\theta, u_2 = a\sin\theta$ so that solutions are defined by

$$p(a^2,\mu,\tau)a = 0 \quad \text{and} \quad q(a^2,\mu,\tau)a = 0. \quad (86)$$

These equations should be viewed as defining a^2 and τ. In view of (75b), the Implicit Function Theorem provides that $q(a^2,\mu,\tau) = 0$ can be solved for $\tau = \tau(a^2,\mu)$, which leaves us with the requirement that

$$g(a,\mu) := p(a^2,\mu,\tau(a^2,\mu))a = r(a^2,\mu)a = 0 \quad (87a)$$

where

$$r(a^2,\mu) := p(a^2,\mu,\tau(a^2,\mu)). \quad (87b)$$

Solutions of $r(z,\mu) = 0$ with $z > 0$ are in one-to-one correspondence with the nontrivial periodic solutions of (1). The function $r(z,\mu)$ can be approximately computed using a combination of Fourier and power series expansions. This can be accomplished using the above formulas, but there are many variants [37, Section 9.4]. Another alternative is based on the 'frequency domain' formulation of the Hopf theory [85], [91], [92].

The existence and number of solutions of (87) near the origin can be investigated in terms of the unfolding parameters of Proposition 6. However, it is also important to identify the stability of periodic solutions. Stability depends on the sign of the first nonzero derivative of $g(a,\mu) = r(a^2,\mu)a$ with respect to a, or equivalently, its unfolding. If we preserve sign by introducing the parameter $\varepsilon = \pm 1$, then

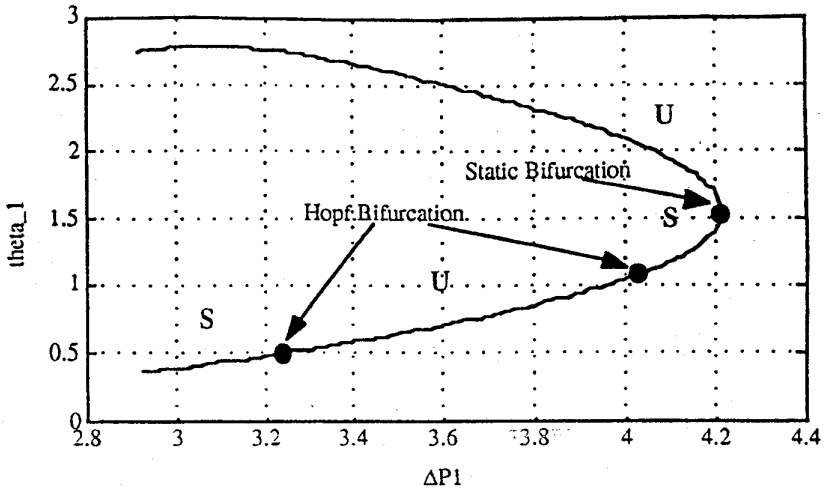

Fig. 14. The bifurcation picture for the four bus, constant admittance system.

the normal forms and unfolding associated with $r(z,\mu)$ are

$$\varepsilon z^k, \text{ and } \gamma_0 + \gamma_1 z + \cdots + \gamma_{k-2} z^{k-2} + \varepsilon z^k \quad \text{for } k \geq 2 \text{ and } \varepsilon = \pm 1 \tag{88}$$

and, hence for $g(a,\mu)$

$$\varepsilon a^{2k-1}, \text{ and } \gamma_0 a + \gamma_1 a^3 + \cdots + \gamma_{k-2} a^{2k-3} + \varepsilon a^{2k-1} \quad \text{for } k \geq 2 \text{ and } \varepsilon = \pm 1. \tag{89}$$

Stability is established by the following proposition.

Proposition 10: Suppose that $(x,\mu) = (0,0)$ is an equilibrium point with a simple pair of imaginary eigenvalues, $\lambda_{1,2} = \pm i$, and with all other eigenvalues having negative real parts. Then the periodic solution corresponding to a pair (a,μ) satisfying $g(a,\mu)$ is asymptotically stable if $D_a g(a,\mu) > 0$ and unstable if $D_a g(a,\mu) < 0$. An equivalent statement in terms of the unfolding is also true.

Proof: This follows from the results of [41, Chap. 8, Section 5] and [37, Section 9.5]. □

Fig. 6 shows the bifurcation diagram for the codimension 1 Hopf bifurcations. The codimension 2 case is illustrated in Fig. 13.

Example 5 Revisited: (Hopf Bifurcation): Let us return to the system of Example 5 with constant admittance loads as characterized by (46). Hopf bifurcations occur in this system as described in [77], [85]. Let us focus on the static bifurcation point at $(\theta_1, \theta_2, \Delta P_1, \Delta P_2) = (1.549, 0.759, 4.216, 2.794)$. The Lyapunov–Schmidt reduction indicates that this bifurcation has codimension 1 and can be efficiently observed in the variable θ_1 and parameter ΔP_1, as illustrated in Fig. 15. We observe the classical saddle node bifurcation.

The curve in Fig. 15 is extended by decreasing ΔP_1. By computing the eigenvalues at equilibria along this curve a dynamic bifurcation point is encountered in [67] at $\Delta P_1 = 4.042$ with damping parameter $\gamma = 0$.[21] Another bifurcation was discovered by further decreasing the parameter ΔP_1. Both are supercritical Hopf bifurcations, so that a stable limit cycle emerges as ΔP_1 increases from 3.244, and as ΔP_1 decreases from 4.042. The above is information summarized in the bifurcation diagram of Fig. 15. Simulation results that show trajectories before and after the lower bifurcation are shown in Figs. 15 and 16. It is interesting to ask about the interaction between the two limit cycles as they move away from the equilibrium point. At the present time such global studies would be carried out by extensive simulation. That has not been done for this example. In general, we expect the global interaction to be quite complex [2].

Table 4 HOPF Bifurcation Points

$C_{12} = 0, C_{13} = 0, C_{23} = 2, B_{12} = 1, B_{13} = B_{23} = .5774$

ΔP_1	ΔP_2	P_1	γ	θ_1	θ_2	ω
4.042	2.887	−1.155	0.00	1.047	.5236	1.2247
4.031	2.876	−1.144	0.05	1.041	.5177	1.2278

In [85], [94] the same system is investigated with positive values of the damping parameter γ. Hopf bifurcations are sought using a variation of the method of [90] and classified using the frequency domain method of [91]. Data comparing the bifurcation points corresponding to $\gamma = 0.0$ and $\gamma = 0.05$ are shown in Table 4.

Remarks: Space precludes more examples on higher codimension bifurcations, but a few comments are in order. Notice that the essential feature of the (codimension 2) generalized Hopf bifurcation (Fig. 11) produces bifurcations involving the birth and death of multiple limit cycles. There are essential four different normal forms (topological distinct phase portraits) for this degeneracy arising from the four possible combinations of signs for ε, γ_0. The other codimension 2 bifurcations of vector fields: the double zero eigenvalue, the imaginary pair and zero eigenvalue, and the

[21] Even though the damping is zero, the system is not conservative because transfer conductances are present [93], [77].

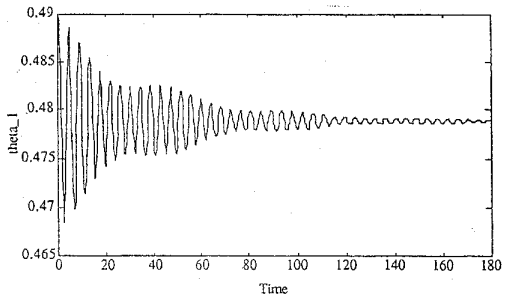

Fig. 15. Simulation just below Hopf bifurcation point ($\Delta P_1 = 3.189$).

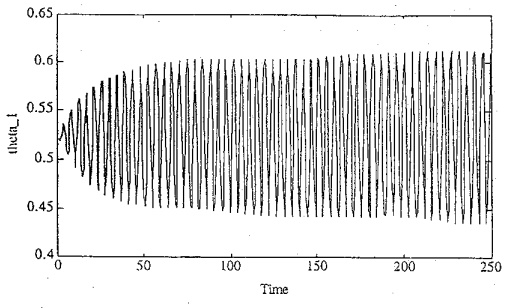

Fig. 16. Simulation just above Hopf bifurcation point ($\Delta P_1 = 3.279$).

two nonresonent imaginary pairs give rise to two, six, and nine topological types, respectively. Each of these types has to be unfolded individually [21].

IV. Concluding Remarks

We have attempted to provide an overview of local bifurcation theory as it is now being applied in power systems analysis. The discussion is based on the general DAE description of power systems which includes classical models and purely differential equation models as a special cases. We have not considered supplemental inequality constraints as they are beyond the scope of the present paper. The formality of our presentation is, in our opinion, necessary partly because terminology is increasingly confused and because much of it may be new to some readers. Hopefully, the geometric perspective that we take is helpful in developing an understanding of the main issues associated with local bifurcation in DAE models of power systems. We have tried to make as many connections as practical to the relevant mathematical and power systems literature.

Clearly, the saddle-node bifurcation has become a widely accepted paradigm for one important form of voltage instability. By far the most prevelent application of the concepts and tools described herein has been to identify the point of collapse—a saddle-node bifurcation point. However, the importance of Hopf bifurcation has been increasingly recognized as it has become clear that stability of the equilibrium can be lost by this mechanism well before reaching the point of collapse. This can be the initial event leading to eventual system failure [2]. Moreover, subcritical Hopf bifurcations can severely constrict the transient stability domain of attraction even before the stability limit is reached.

Higher codimension bifurcations have drawn only limited attention even though they are clearly present in early parametric studies [3] of power system equilibria and more recent studies of Hopf bifurcation [88]. The prevailing attitude is that the practical significance of a bifurcation diminishes with increasing codimension. Nevertheless, multiparameter problems, such as Example 6, are intrinsically important in power system operations and issues involving higher codimension bifurcations will certainly emerge.

We have, by necessity, left out some interesting and important topics. Among them is the issue of proximity indices that measure nearness to collapse and their application to voltage control. Many proposed indices have been based on the presumption of a saddle-node bifurcation (or, at least, a singular Jacobian) as the collapse mechanism [95]–[97]. Also, aspects of computing technology, like sparsity, that are particularly important for very large systems and routinely included as part of conventional power engineering analysis have not been addressed.

Nor have we discussed specific software packages for power system bifurcation analysis. We might note that several papers dealing with small scale power systems cite application of the general bifurcation analysis package AUTO [98]. As can be seen from our references, many research groups have built special purpose software for performing a limited bifurcation analysis on power systems of moderate to very large scale.

Some of the computational methods that we have described invite the integration of numerical and symbolic processing. In [14] the use of Macsyma to implement the Lyapunov–Schmidt reduction is noted. One aspect of symbolic manipulation is the assembly of power system models and code generation for the more elaborate numerical algorithms, i.e., the Newton–Raphson–Seydel method for computing near bifurcation points. This modeling process along with the Lyapunov–Schmidt reduction was implemented in PROLOG [67] and used to investigate small (up to 10 bus) systems. A recent effort aimed at applying symbolic tools to larger (up to 118 bus) systems is described in [99].

References

[1] F. M. A. Salam, J. E. Marsden, and P. P. Varaiya, "Arnold diffusion in the swing equations of power systems," *IEEE Trans. Circ. and Syst.*, vol. CAS-31, pp. 673–688, 1984.

[2] H. O. Wang, E. H. Abed, and A. M. A. Hamden, "Bifurcation, chaos, and crisis in voltage collapse of a model power system," *IEEE Trans. Circ. and Syst.—I: Fundamental Theory and Applic.*, vol. 41, pp. 294–302, 1994.

[3] C. J. Tavora and O. J. M. Smith, "Equilibrium analysis of power systems," *IEEE Trans. Power Applic. and Syst.*, vol. PAS-91, pp. 1131–1137, 1972.

[4] ——, "Stability analysis of power systems," *IEEE Trans. Power Apparatus and Syst.*, vol. PAS-91, pp. 1138–1144, 1972.

[5] A. J. Korsak, "On the question of uniqueness of stable load-flow solutions," *IEEE Trans. Power Apparatus and Syst.*, vol. PAS-91, pp. 1093–1100, 1972.

[6] V. A. Venikov, V. A. Stroev, V. I. Idelchick, and V. I. Tarasov, "Estimation of power system steady-state stability in load flow calculations," *IEEE Trans. Power Apparatus and Syst.*, vol. PAS-94, pp. 1034–1038, 1975.
[7] T. Van Cutsem, "'Voltage collapse mechanisms' a case study," in *Proc. Bulk Power Syst. Voltage Phenomena II: Voltage Stability and Security*, Deep Creek Lake, MD: ECC, Inc., 1991, pp. 85–101.
[8] K. T. Vu and C.-C. Liu, "Shrinking stability regions and voltage collapse in power systems," *IEEE Trans. Circ. and Syst.-I, Fund. Theory and Applic.*, vol. 39, pp. 271–289, 1992.
[9] D. J. Hill, "Nonlinear dynamic load models with recovery for voltage stability studies," *IEEE Trans. Power Syst.*, vol. 4, pp. 166–176, 1993.
[10] J. V. Milanovic and I. A. Hiskens, "Effects of load dynamics on power system damping," *IEEE Trans. Power Syst.*, vol. 10, pp. 1022–1027, 1995.
[11] T. Van Cutsem, "An approach to corrective control of voltage instability using simulation and sensitivity," *IEEE Trans. Power Syst.*, vol. 10, pp. 616–622, 1995.
[12] M. A. Pai, P. W. Sauer, B. C. Lesieutre, and R. Adapa, "Structural stability in power systems-effect of load models," *IEEE Trans. Power Syst.*, vol. 10, pp. 609–615, 1995.
[13] C. L. DeMarco and A. R. Bergen, "Applications of singular perturbation techniques to power system transient stability analysis," in *Proc. IEEE Int. Symp. on Circ. and Syst.*, 1984, pp. 597–601.
[14] H. G. Kwatny, A. K. Pasrija, and L. Y. Bahar, "Static bifurcations in electric power networks: Loss of steady state stability and voltage collapse," *IEEE Trans. Circ. and Syst.*, vol. CAS-33, pp. 981–991, 1986.
[15] I. Dobson and H.-D. Chiang, "Toward a theory of voltage collapse in electric power systems," *Syst. and Contr. Lett.*, vol. 13, pp. 253–262, 1989.
[16] I. Dobson, "Observations on geometry of saddle node bifurcation and voltage collapse in electric power systems," *IEEE Trans. Circ. and Syst., Part I*, vol. 39, pp. 240–243, 1992.
[17] J. H. Chow, "Time-Scale modeling of dynamic networks with applications to power systems," in *Lecture Notes in Control and Information Sciences*, vol. 46. New York: Springer-Verlag, 1982.
[18] V. Venkatasubramanian, H. Schättler, and J. Zaborszky, "A taxonomy of the dynamics of the large power system with emphasis on its voltage stability," in *Proc. Bulk Power Syst. Voltage Phenomena II: Voltage Stability and Security*, Deep Creek Lake, MD: 1991, pp. 9–44.
[19] M. W. Hirsch and S. Smale, *Differential Equations, Dynamical Systems, and Linear Algebra*. New York: Academic, 1974.
[20] K. E. Brenan, S. L. Campbell, and L. R. Petzold, *Numerical Solution of Initial-Value Problems in Differential-Algebraic Equations*. New York: Elsevier, 1989.
[21] J. Guckenheimer and P. Holmes, *Nonlinear Oscillations, Dynamical Systems, and Bifurcation of Vector Fields*. New York: Springer-Verlag, 1983.
[22] W. M. Boothby, *An Introduction to Differentiable Manifolds and Riemannian Geometry*. San Diego: Academic, 1986.
[23] L. O. Chua and H. Oka, "Normal forms for constrained nonlinear differential equations, Part I: Theory," *IEEE Trans. Circ. and Syst.*, vol. 35, pp. 881–901, 1988.
[24] I. Hiskins and D. J. Hill, "Energy functions, transient stability and voltage behavior in power systems with nonlinear loads," *IEEE Trans. Power Syst.*, vol. 4, pp. 1525–1533, 1989.
[25] V. Venkatasubramanian, H. Schättler, and J. Zaborszky, "Voltage dynamics: Study of a generator with voltage control, transmission, and matched MW load," *IEEE Trans. Autom. Contr.*, vol. 37, pp. 1717–1733, 1992.
[26] B. K. Johnson, "Extraneous and false load flow solutions," *IEEE Trans. Power Apparatus and Syst.*, vol. PAS-96, p. 524, 1977.
[27] H. Glavitsch, "Where developments in power system stability should be directed," in *Proc. Int. Symp. on Power System Stability*, Ames, IA, 1985, pp. 61–68.
[28] I. A. Hiskins and D. J. Hill, "Failure modes of a collapsing power system," in *Proc. Bulk Power Syst. Voltage Phenomena II: Voltage Stability and Security*, Deep Creek Lake, MD, 1991, pp. 53–63.
[29] S. E. M. de Oliveira, "Synchronizing and damping torque coefficients and power system steady state stability as affected by static VAR compensators," *IEEE Trans. Power Syst.*, vol. 9, pp. 109–119, 1994.
[30] C. A. Cañizares, "On bifurcations, voltage collapse and load modeling," *IEEE Trans. Power Syst.*, vol. 10, pp. 512–518, 1995.
[31] V. I. Arnold, *Geometrical Methods in the Theory of Ordinary Differential Equations*. New York: Springer-Verlag, 1983.
[32] R. A. Schlueter, I. P. Hu, and T. Y. Guo, "Dynamic/static voltage stability security criteria," in *Proc. Bul. Power System Voltage Stability Phenomena II: Voltage Stability and Security*, Deep Creek Lake, MD: ECC, Inc., 1991, pp. 265–303.
[33] T. Guo and R. A. Schlueter, "Identification of generic bifurcation and stability problems in power system differential-algebraic model," *IEEE Trans. Power Syst.*, vol. 9, pp. 1032–1038, 1994.
[34] D. K. Arrowsmith and C. M. Place, *An Introduction to Dynamical Systems*. Cambridge, UK: Cambridge Univ. Press, 1990.
[35] J. K. Hale, *Ordinary Differential Equations*. New York: Wiley, 1969.
[36] J. Hale and H. Koçak, *Dynamics and Bifurcations*. New York: Springer-Verlag, 1991.
[37] S. N. Chow and J. K. Hale, *Methods of Bifurcation Theory*. New York: Springer-Verlag, 1982.
[38] M. W. Hirsch, *Differential Topology*. New York: Springer-Verlag, 1976.
[39] M. Golubitsky and V. Guilleman, *Stable Mappings and Their Singularities*. New York: Springer-Verlag, 1973.
[40] R. Gilmore, *Catastrophe Theory for Scientists and Engineers*. New York: Wiley, 1981.
[41] M. Golubitsky and D. G. Schaeffer, *Singularities and Groups in Bifurcation Theory: Vol. 1*. New York: Springer-Verlag, 1984.
[42] J. Berg and H. G. Kwatny, "A canonical parameterization of the Kronecker form of a matrix pencil," *Automatica*, vol. 31, pp. 669–680, 1995.
[43] F. R. Gantmacher, *The Theory of Matrices*, vol. 1. New York: Chelsea, 1959.
[44] J. M. T. Thomson and G. W. Hunt, *Elastic Instability Phenomena*. New York: Wiley, 1984.
[45] M. M. Begovic and A. G. Phadke, "Dynamic simulation of voltage collapse," *IEEE Trans. Power Syst.*, vol. 5, pp. 198–203, 1990.
[46] M. Kubicek, "Dependence of systems of nonlinear equations on a parameter," *ACM Trans. Mathematical Software*, vol. 2, pp. 98–107, 1976.
[47] R. Seydel, "Numerical computation of branch points in nonlinear equations," *Numerische Mathematik*, vol. 33, pp. 339–352, 1979.
[48] V. Ajjarapu, "Identification of steady-state voltage stability in power systems," *Int. J. Energy Syst.*, vol. 11, pp. 43–46, 1991.
[49] F. L. Alvarado and T. H. Jung, "Direct detection of voltage collapse conditions," in *Proc. Bulk Power Syst. Voltage Phenomena-Voltage Stability and Security*, EPRI, 1988, pp. 5.23–5.38.
[50] C. A. Cañizares and F. L. Alvarado, "Computational experience with the point of collapse method on very large AC/DC systems," in *Proc. Bulk Power Syst. Voltage II Phenomena-Voltage Stability and Security*, Deep Creek Lake, MD: 1991, pp. 103–112.
[51] E. G. Carpaneto, G. Chicco, R. Napoli, and F. Piglione, "A Newton-Raphson method for steady-state voltage stability assessment," *Proc. Bulk Power Syst. Voltage II Phenomena-Voltage Stability and Security*, Deep Creek Lake, MD: 1991, pp. 341–345.
[52] K. Iba, H. Suzuki, M. Egawa, and T. Watanabe, "Calculation of critical loading with nose curve using homotopy continuation method," *IEEE Trans. Power Syst.*, vol. 6, pp. 584–590, 1991.
[53] Y. Kataoka, "An approach for the regularization od a power flow solution around the maximum loading point," *IEEE Trans. Power Syst.*, vol. 7, pp. 1068–1077, 1992.
[54] T. Wu and R. Fischl, "Identification of load flow feasibility region in megawatt transfer space," in *Proc. 24th Annu. North Amer. Power Symp.*, Reno, NV, 1992, pp. 226–233.
[55] C. A. Cañizares and F. L. Alvarado, "Point of collapse and continuation methods for large AC/DC systems," *IEEE Trans. Power Syst.*, vol. 8, pp. 1–7, 1993.
[56] H.-D. Chiang, A. J. Fluek, K. S. Shah, and N. Balu, "CPFLOW: A practical tool for tracing power system steady-state stationary behavior due to load and generation variations," *IEEE Trans. Power Syst.*, vol. 10, pp. 623–630, 1995.

[57] I. Dobson and L. Lu, "Computing an optimal direction in control space to avoid saddle node bifurcation and voltage collapse in electric power systems," *IEEE Trans. Autom. Contr.*, vol. 37, pp. 1616–1620, 1992.
[58] R. Jean-Jumeau and H.-D. Chiang, "Parameterizations of the load-flow equations for eliminating ill-conditioning load flow solutions," *IEEE Trans. Power Syst.*, vol. 8, pp. 1004–1011, 1993.
[59] ——, "A more efficient formulation for computation of the maximum loading points in electric power systems," *IEEE Trans. Power Syst.*, vol. 10, pp. 635–641, 1995.
[60] W. H. Press, B. P. Flannery, S. A. Teukolsky, and W. T. Vettering, *Numerical Recipes: The Art of Scientific Computing*. New York: Cambridge, 1986.
[61] R. Wait, *The Numerical Solution of Algebraic Equations*. New York: Wiley, 1979.
[62] J. M. Ortega and W. C. Rheinboldt, *Iterative Solutions of Nonlinear Equations in Several Variables*. New York: Academic, 1970.
[63] E. Wasserstrom, "Numerical solutions by the continuation method," *SIAM Rev.*, vol. 15, pp. 89–119, 1973.
[64] V. A. Ajjarapu and C. Christy, "The continuation power flow: A tool for steady-state voltage stability analysis," *IEEE Trans. Power Syst.*, vol. 7, pp. 416–423, 1992.
[65] R. J. Thomas, R. D. Barnard, and J. Meisel, "The generation of quasi steady-state load flow trajectories and multiple singular point solutions," *IEEE Trans. Power Apparatus and Syst.*, vol. 90, pp. 1967–1974, 1971.
[66] J. Jarjis and F. D. Galiana, "Quantitative analysis of steady state stability in power networks," *IEEE Trans. Power Apparatus and Syst.*, vol. PAS-100, pp. 318–326, 1981.
[67] X. M. Yu, "Stability and bifurcation of equilibria in electric power networks," Ph.D. dissertation, Drexel Univ., Philadelphia, 1991.
[68] I. Dobson and L. Lu, "Using an iterative method to compute a closest saddle node bifurcation in the load parameter space of an electric power system," in *Proc. Bulk Power Syst. Voltage II Phenomena-Voltage Stability and Security*, Deep Creek Lake, MD, 1991, pp. 157–161.
[69] H. G. Kwatny, "Stability enhancement via secondary voltage regulation," in *Proc. Bulk Power Syst. Voltage Phenomena II: Voltage Stability and Security*, Deep Creek Lake, MD, ECC, Inc., 1991, pp. 147–155.
[70] I. Dobson and L. Lu, "New methods for computing a closest saddle-node bifurcation and worst case load power margin for voltage collapse," *IEEE Trans. Power Syst.*, vol. 8, pp. 905–913, 1993.
[71] J. Lu, C. W. Liu, and J. S. Thorp, "New methods for computing a saddle-node bifurcation point for voltage stability analysis," *IEEE Trans. Power Syst.*, vol. 10, pp. 978–985, 1995.
[72] V. I. Arnold, V. V. Kozlov, and A. I. Neishtadt, *Mathematical Aspects of Classical and Celestial Mechanics*. Heidelberg: Springer-Verlag, vol. 3, 1988.
[73] IEEE, "Voltage stability of power systems: Concepts, tools and industry experience," in *IEEE Syst. Dynamic Perf. Subcommittee Rep. 90TH0358-2-PWR*, New York, 1990.
[74] J. LaSalle and S. Lefschetz, *Stability by Liapunov's Direct Method*. New York: Academic, 1961.
[75] Y. Tamura, H. Mori, and S. Iwamoto, "Relationship between voltage instability and multiple load flow solutions in electric power systems," *IEEE Trans. Power Apparatus and Syst.*, vol. PAS-102, pp. 1115–1125, 1983.
[76] S. Abe, N. Hamada, A. Isono, and K. Okuda, "Load flow convergence in the vicinity of a voltage instability limit," *IEEE Trans. Power Apparatus and Syst.*, vol. PAS-97, pp. 1983–1993, 1978.
[77] H. G. Kwatny and X. M. Yu, "Energy analysis of load-induced flutter instability in classical models of electric power networks," *IEEE Trans. Circ. and Syst.*, vol. 36, pp. 1544–1557, 1989.
[78] J. Baillieul and C. I. Byrnes, "Geometric critical point analysis of lossless power system models," *IEEE Trans. Circ. and Syst.*, vol. CAS-29, pp. 724–737, 1982.
[79] P. W. Sauer, R. J. Evans, and M. A. Pai, "Maximum unconstrained loadability of power systems," in *Proc. 1990 PICA Conf.*, 1990, pp. 1818–1821.
[80] T. Wu and R. Fischl, "Load flow feasibility region region identification in inter-area real power import space," in *Proc. 11th Power Syst. Computation Conf.*, Avignon, France, 1993, pp. 181–188.
[81] S. Wunderlich, T. Wu, R. Fischl, and R. O'Connell, "An inter-area transmission and voltage limitation (TVLIM) program," *IEEE Trans. Power Syst.*, vol. 10, pp. 1257–1263, 1995.
[82] J. E. van Ness, F. M. Brash Jr., G. L. Landgren, and S. I. Neuman, "Analytic investigation of dynamic instability occuring at powerton station," *IEEE Trans. Power Apparatus and Syst.*, vol. PAS-99, pp. 1386–1395, 1980.
[83] E. Abed and P. Varaiya, "Nonlinear oscillations in power systems," *Int. J. Electric Power and Energy Syst.*, vol. 6, pp. 37–43, 1984.
[84] J. C. Alexander, "Oscillatory solutions of a model system of nonlinear swing equations," *Int. J. Electric Power and Energy Syst.*, vol. 8, pp. 130–136, 1986.
[85] H. G. Kwatny and G. E. Piper, "Frequency domain analysis of Hopf bifurcations in electric power networks," *IEEE Trans. Circ. and Syst.*, vol. 37, pp. 1317–1321, 1990.
[86] C. Rajagopalan, P. W. Sauer, and M. A. Pai, "An integrated approach to dynamic and static voltage stability," in *Proc. Amer. Contr. Conf.*, 1989, pp. 1231–1236.
[87] M. R. Iravani and A. Semlyen, "Hopf bifurcations in torsional dynamics," *IEEE Trans. Power Syst.*, vol. 7, pp. 28–35, 1992.
[88] R. L. Chen and P. Varaiya, "Degenerate Hopf bifurcation in power systems," *IEEE Trans. Circ. and Syst.*, vol. CAS-35, pp. 818–824, 1988.
[89] H. D. Chiang *et al.*, "Chaos in a simple power system," *IEEE Trans. Power Syst.*, vol. 8, pp. 1407–1414, 1993.
[90] D. Roose and V. Hlavacek, "A direct method for the computation of Hopf bifurcation points," *SIAM J. Applied Mathematics*, vol. 45, pp. 879–894, 1985.
[91] A. I. Mees and L. Chua, "The Hopf bifurcation theorem and its applications to nonlinear oscillations in circuits and systems," *IEEE Trans. Circ. and Syst.*, vol. 26, pp. 235–254, 1979.
[92] J. Moiola and G. Chen, "Computations of limit cycles via higher order harmonic balance approximations," *IEEE Trans. Autom. Contr.*, vol. 38, pp. 782–790, 1993.
[93] H. G. Kwatny, L. Y. Bahar, and A. K. Pasrija, "Energy-like Lyapunov functions for power system stability analysis," *IEEE Trans. Circ. and Syst.*, vol. CAS-32, pp. 1140–1149, 1985.
[94] G. E. Piper, "Limit cycle analysis of multivariable nonlinear dynamic systems," Ph.D. dissertation, Drexel Univ., Philadelphia, PA, 1990.
[95] A. Tiranuchit and R. J. Thomas, "A posturing strategy against voltage instabilities in electric power systems," *IEEE Trans. Power Syst.*, vol. 3, pp. 87–93, 1988.
[96] P.-A. Löf, G. Andersson, and D. J. Hill, "Voltage stability indices for stressed power systems," *IEEE Trans. Power Syst.*, vol. 8, pp. 326–332, 1993.
[97] M. M. Begovic and A. G. Phadke, "Control of voltage stability using sensitivity analysis," *IEEE Trans. Power Syst.*, vol. 7, pp. 114–120, 1992.
[98] E. J. Doedel, "AUTO: A program for the automatic bifurcation analysis of autonomous systems," *Cong. Num.*, vol. 30, pp. 265–284, 1981.
[99] H. G. Kwatny, X. M. Yu, and C. Nwankpa, "Local bifurcation analysis of power systems using MATLAB," in *Proc. 4th IEEE Conf. on Contr. Applic.*, Albany, IEEE, 1995, pp. 57–62.

Harry G. Kwatny (Senior Member, IEEE) received the B.S.M.E. degree from Drexel Institute of Technology in 1961, the S.M. degree in aeronautics and astronautics from the Massachusetts Institute of Technology in 1962 and the Ph.D. degree in electrical engineering from the University of Pennsylvania in 1967.

He is currently the S. Herbert Raynes Professor of Mechanical Engineering at Drexel University, Philadelphia, PA. His main research interests include the analysis and control of parameter dependent nonlinear dynamics and the use of combined numeric-symbolic computation for addressing these problems. He also has a strong interest in physical system modeling, analysis and control of power plants and power systems, flexible spacecraft and space robotics, flight control, ground vehicle dynamics, and structural acoustics control.

Robert F. Fischl (Life Fellow, IEEE) was born in Prague, Czechoslovakia, in 1931. He received the B.S.E.E. degree from the City College of New York in 1956 and the M.S. and Ph.D. degrees in electrical engineering from the University of Michigan, Ann Arbor, MI, in 1958 and 1966, respectively.

From 1956 to 1996 he was a Researcher at Willow Run and Cooley Electronics Laboratories at the University of Michigan. In 1966 he joined the faculty of Drexel University, where he is currently a Professor of Electrical Engineering and Director of the Center of Electric Power Engineering. His research interests are in the areas of power systems and power electronics circuits design. His recent work has been in the areas of voltage collapse and the application of data fusion and artifical neural networks to power system security assessment and enhancement.

Dr. Fischl is a member of Eta Kappa Nu and Tau Beta Pi.

Chika O. Nwankpa (Member, IEEE) was born in Owerri, Nigeria, in 1962. He received the Magistr Diploma in electric power systems from Leningrad Polytechnical Institute, USSR, in 1986. He received the Ph.D. degree in electrical and computer engineering from Illinois Institute of Technology in 1990.

He is currently an Associate Professor in the Electrical and Computer Engineering Department at Drexel University. His research interests are in power systems dynamics and effects of uncertanties in their modeling. He is involved in work in the field of high power switching.

Dr. Nwankpa received the 1991 NSF Engineering Research Initiation Award and a 1994 Presidential Faculty Fellow (PFF) Award.